Ageing Research Reviews 94 (2024) 102197

Contents lists available at ScienceDirect

Ageing Research Reviews

journal homepage: www.elsevier.com/locate/arr

Review article

In vivo imaging of synaptic density in neurodegenerative disorders with positron emission tomography: A systematic review

Malouke Visser [a,b], John T. O'Brien [a], Elijah Mak [a,*]

[a] Department of Psychiatry, School of Clinical Medicine, Addenbrooke's Hospital, University of Cambridge, United Kingdom
[b] Neuropsychology and Rehabilitation Psychology, Donders Institute for Brain, Cognition and Behaviour, Radboud University, Nijmegen, the Netherlands

ARTICLE INFO

Keywords:
Aging
Dementia
SV2A
PET
Synaptic density
Neurodegeneration

ABSTRACT

Positron emission tomography (PET) with radiotracers that bind to synaptic vesicle glycoprotein 2 A (SV2A) enables quantification of synaptic density in the living human brain. Assessing the regional distribution and severity of synaptic density loss will contribute to our understanding of the pathological processes that precede atrophy in neurodegeneration. In this systematic review, we provide a discussion of *in vivo* SV2A PET imaging research for quantitative assessment of synaptic density in various dementia conditions: amnestic Mild Cognitive Impairment and Alzheimer's disease, Frontotemporal dementia, Progressive supranuclear palsy and Corticobasal degeneration, Parkinson's disease and Dementia with Lewy bodies, Huntington's disease, and Spinocerebellar Ataxia. We discuss the main findings concerning group differences and clinical-cognitive correlations, and explore relations between SV2A PET and other markers of pathology. Additionally, we touch upon synaptic density in healthy ageing and outcomes of radiotracer validation studies. Studies were identified on PubMed and Embase between 2018 and 2023; last searched on the 3rd of July 2023. A total of 36 studies were included, comprising 5 on normal ageing, 21 clinical studies, and 10 validation studies. Extracted study characteristics were participant details, methodological aspects, and critical findings. In summary, the small but growing literature on *in vivo* SV2A PET has revealed different spatial patterns of synaptic density loss among various neurodegenerative disorders that correlate with cognitive functioning, supporting the potential role of SV2A PET imaging for differential diagnosis. SV2A PET imaging shows tremendous capability to provide novel insights into the aetiology of neurodegenerative disorders and great promise as a biomarker for synaptic density reduction. Novel directions for future synaptic density research are proposed, including (a) longitudinal imaging in larger patient cohorts of preclinical dementias, (b) multi-modal mapping of synaptic density loss onto other pathological processes, and (c) monitoring therapeutic responses and assessing drug efficacy in clinical trials.

1. Introduction

Neurodegenerative disorders are a complex and pressing challenge in the field of neuroscience, demanding advanced diagnostic and monitoring techniques. A key element of neuropathology in neurodegenerative disorders is the selective loss of vulnerable populations of neurons, which plays a central role in disease progression (Dugger and Dickson, 2017). While magnetic resonance imaging (MRI) and computed tomography (CT) are capable of detecting grey matter (GM) atrophy at a macroscale level, structural imaging modalities lack the sensitivity to assess the majority of pathological processes *preceding* neuronal loss (Dugger and Dickson, 2017; Serrano et al., 2022; Topcuoglu et al., 2022b).

In response to this challenge, positron emission tomography (PET) has emerged as a powerful tool. PET enables more specific, *in vivo*, imaging and quantification of a wide range of physiological functions at the molecular level, including the presence of specific protein aggregates associated with neurodegeneration, such as β-amyloid, tau, and α-synuclein. This has proven invaluable in providing insights for differential diagnostics and therapeutic monitoring (Carson et al., 2022; Dierckx et al., 2021; Herholz et al., 2007; Iaccarino et al., 2017; Topcuoglu et al., 2022a; van Waarde et al., 2021).

Among the multitude of valuable pathology markers, *synaptic density* has recently gained considerable attention from the scientific

* Correspondence to: Department of Psychiatry, University of Cambridge School of Clinical Medicine, Box 189, Level E4 Cambridge Biomedical Campus, Cambridge CB2 0SP, United Kingdom.
E-mail address: fkm24@cam.ac.uk (E. Mak).

https://doi.org/10.1016/j.arr.2024.102197
Received 17 November 2023; Received in revised form 9 January 2024; Accepted 12 January 2024
Available online 22 January 2024

community (Becker et al., 2020; Cai et al., 2019; van Waarde et al., 2021). A growing body of evidence demonstrates the significance of synapse dysfunction in neurodegenerative disorders, resulting in the emerging theory that many of these conditions can be categorised as *synaptopathies* (Lepeta et al., 2016; Luo et al., 2018; Rabiner, 2018; Serrano et al., 2022). Measuring synaptic density within specific brain regions is not a novel concept. Conventional synaptophysin-based methods include stereology, immunohistochemistry, and electron microscopy (Calhoun et al., 1996). However, such methods entail *ex vivo* measurements and are thus limited by the requirement of post-mortem or surgically resected brain tissue (Finnema et al., 2016; Serrano et al., 2022).

Recently, the development of high-affinity PET radiopharmaceuticals targeting the synaptic vesicle protein 2 A (SV2A) has enabled the ability to directly assess synaptic density in the living human brain (Finnema et al., 2016; Mercier et al., 2014; Mercier et al., 2017). SV2A is a glycoprotein present in presynaptic vesicles of both glutamatergic and GABAergic neurons throughout the central nervous system. Its ubiquitous expression has led researchers to propose SV2A as a proxy for synaptic density (Cai et al., 2019; Carson et al., 2022; Finnema et al., 2016; Serrano et al., 2022). Traditionally linked to epilepsy, SV2A serves as the target for antiepileptic drugs levetiracetam (Keppra®) and brivaracetam (Briviact®, Feng et al., 2009; Gillard et al., 2011; Lynch et al., 2004).

Utilising SV2A PET imaging as a potential indicator of synaptopathology, researchers can gain insights into the dynamics of synaptic density, revealing patterns of abnormality (Finnema et al., 2016; Finnema et al., 2020; Rizzoli and Betz, 2005). Consequently, these findings may pave the way for the development and assessment of new therapeutic interventions aimed at reducing synaptic toxicity. While previous narrative reviews have outlined the development, radiochemistry, and application of SV2A PET imaging agents for measuring synaptic density *in vivo* in neuropsychiatric and neurodegenerative disorders, a systematic approach in this area has yet to be undertaken (Becker et al., 2020; Cai et al., 2019; Carson et al., 2022; Martin et al., 2023; Rabiner, 2018). Here we report what is, to our knowledge, the first systematic review of SV2A PET imaging research for quantitative assessment of synaptic density in neurodegenerative disorders. Providing an objective synthesis of existing evidence, we enable a comprehensive evaluation of the current state of research, thereby aiming to illuminate the importance of SV2A PET in understanding neurodegenerative pathology.

2. Methods

This systematic review was reported following the guidelines of the Preferred Reporting Items for Systematic Reviews and Meta-analyses (Page et al., 2021).

2.1. Search strategy and selection criteria

To identify relevant studies involving PET imaging of synaptic density in dementia patients, a search was conducted in PubMed and Embase, using the following search terms: ((Positron emission tomography OR PET) AND (Synaptic density OR presynaptic density OR synaptic loss OR synaptic damage OR synaptic complexity OR UCB-J OR UCB-H OR SV2A) AND (Dementia OR Neurodegeneration OR Alzheimer disease OR Lewy body OR Parkinson disease OR Frontotemporal OR Huntington OR Progressive supranuclear palsy OR Corticobasal degeneration OR Primary tauopathies OR Mild cognitive impairment OR Normal aging OR Healthy aging OR Carriers OR Presymptomatic OR Asymptomatic OR Validation OR Test retest)). The complete search strings are reported in the supplemental materials (Table S1). The initial search was conducted by one author (M.V.) on the 19th of June 2023. Applied filters were language (English), peer-reviewed literature, and publication date (from January 2019). On the 3rd of July 2023, the search was extended up to January 2018. Inclusion criteria encompassed studies that investigated synaptic density *in vivo* using PET imaging in the following populations: (1) healthy ageing individuals; (2) individuals with a family history of dementia; (3) carriers of dementia-associated risk genes, or; (4) patients diagnosed with a neurodegenerative disorder. Additionally, studies addressing methodological aspects of synaptic density PET imaging, specifically those aimed at validation, were also included. Excluded from considerations were case reports, reviews, letters, commentaries, and editorials. Furthermore, if multiple papers covered the same sample, the most recent study was considered the primary source to prevent duplication.

2.2. Study selection

After duplicate removal, a single author (M.V.) conducted the selection process by reviewing the titles and abstracts of the search results. Studies were classified as “Include” (eligible), “Maybe” (potentially eligible), or “Exclude” (not eligible) based on their relevance. Full texts were then obtained for further assessment of eligibility. Any uncertainty regarding study selection was resolved through a consensus-based discussion with a second reviewer (E.M.). For transparency, rationales for exclusion after full-text screening was documented in the supplemental materials (Table S2). To ensure comprehensive literature coverage, references cited in the included study reports were reviewed to identify additional relevant studies. The PRISMA flow diagram in Fig. 1 provides a visual summary of the study selection process.

2.3. Data extraction, risk of bias assessment and data synthesis

M.V. extracted the following study characteristics: (1) Participant details: disorder, sample size, time points (if applicable), age, and sex distribution; (2) Methodological aspects: study type, imaging specifics (i.e., modality and acquisition, radioligand used, reference region); and (3) Results: principal findings relating to group comparisons (regional and global), correlations with other pathology markers and cognitive performance. The results were presented in a table, a figure, and described in narrative form. No attempts were made to extract quantitative data for meta-analysis.

3. Results

The database search resulted in 200 studies. Seven studies were identified through citation screening. Following careful evaluation, 36 key studies published between 2018 and 2023 were included in the systematic review (see flow diagram in Fig. 1). Included studies were focused normal ageing ($n = 5$), individuals with cognitive impairment and various neurodegenerative conditions ($n = 21$), and validation studies on determining suitable quantification methods of SV2A expression and evaluating the kinetic properties of radiotracers ($n = 10$). Clinical studies included patients on amnestic Mild Cognitive Impairment (aMCI) and Alzheimer’s disease (AD, $n = 9$), Frontotemporal dementia behavioural variant (bvFTD, $n = 2$), Progressive supranuclear palsy (Richardson’s syndrome; PSP) and CBS (Corticobasal syndrome without Alzheimer’s pathology, otherwise referred to as Corticobasal degeneration; CBD, $n = 4$), Parkinson’s disease (PD) and dementia with Lewy bodies (DLB, $n = 4$), Huntington’s disease (HD, $n = 1$), and Spinocerebellar Ataxia Type 3 (SCA3, $n = 1$). A summary of the clinical study characteristics and principal findings, grouped by publication date and neurodegenerative disorder, is described in Table 1. Key findings will be interpreted and discussed in further detail in Section 4.3.

Clinical study methods exhibited some notable commonalities and differences. Approximately half of the studies ($n = 10$) included a sample size of 20 or more subjects with a neurodegenerative disorder. The majority of studies ($n = 16$) exclusively used cross-sectional data while there were five longitudinal studies across aMCI ($n = 1$), AD ($n = 1$), PSP and CBS ($n = 1$), and PD ($n = 2$).

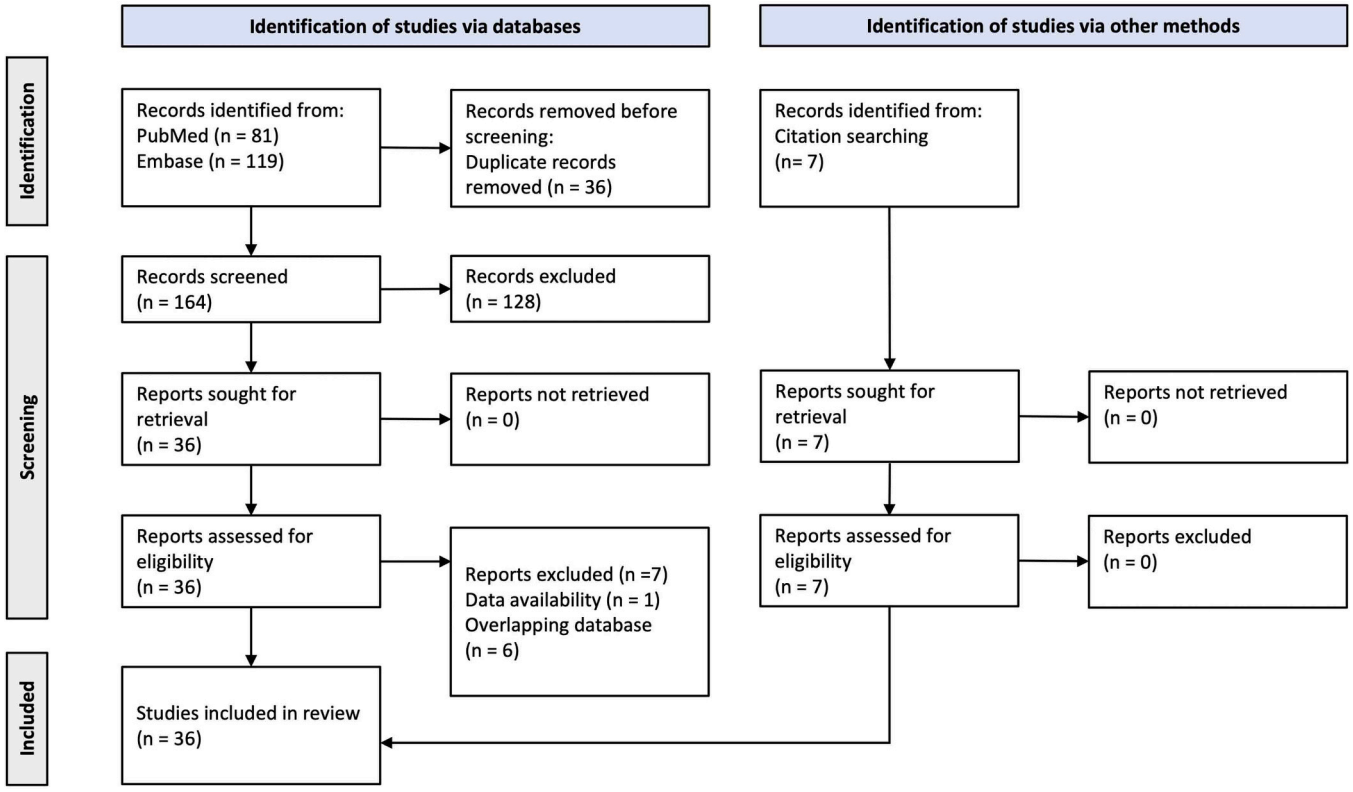

Fig. 1. PRISMA flow diagram of the literature search **(filename = Fig. 1.colourised_M.Visser)** *Notes.* Adapted from Page et al. (2021).

All studies integrated T1-weighted MRI scanning to control for cases with anatomical abnormalities, facilitate co-registration with PET data and define regions of interest if applicable. PET imaging data was largely captured dynamically ($n = 16$), but studies utilised different types of PET machines (PET ($n = 7$), PET-CT ($n = 7$), or PET-MR scanners ($n = 7$)). The predominant tracer choice was [^{11}C]UCB-J ($n = 17$), while a smaller number of studies selected relatively novel tracers [^{18}F]UCB-H ($n = 2$) and [^{18}F]SynVesT-1 ($n = 2$). Moreover, a notable diversity was observed in the methods employed to quantify the PET binding signal, with nondisplaceable binding potential (BP_{ND}) being the prevailing metric in $n = 8$ studies. Followed by standardised uptake value ratio (SUVR $n = 3$, SUVR-1 $n = 3$), distribution volume ratio (DVR_{CBL} $n = 3$, DVR_{SO} $n = 1$), and volume of distribution (V^T, $n = 3$). A limited number of studies ($n = 4$) employed arterial cannulation to obtain the arterial input function (AIF). In contrast, most studies ($n = 17$) opted for non-invasive alternatives for arterial sampling. This encompassed the application of simplified reference tissue modelling ($n = 9$), the calculation of SUVR ($n = 6$), and the implementation of image-derived input functions (IDIF, $n = 2$; both in the [^{18}F]UCB-H tracer studies).

With regards to statistical analysis, a large number of studies ensured that experimental groups were matched for age ($n = 18$) and sex ($n = 15$), however relatively few described efforts to match for education ($n = 9$). Two studies did not make direct comparisons between groups (Coomans et al., 2021; Mecca, O'Dell et al., 2022). To correct for multiplicity, studies mostly applied FDR ($n = 9$), but FWE ($n = 4$) and Bonferroni ($n = 3$) correction methods were also conducted. Additionally, two studies did not report which correction method was used (Chen et al., 2018; Matuskey et al., 2020), one study employed both FDR and FWE (Malpetti et al., 2023), and two studies exclusively reported uncorrected results (Coomans et al., 2021; Venkataraman et al., 2022). All but two study corrected for Partial Volume Effects (PVEs, Coomans et al., 2021; Wilson et al., 2020). Applied voxel-based Partial Volume Correction (PVC) methods were the Muller-Gartner method (MG, $n = 5$), the Iterative Yang algorithm (IY, $n = 5$), and the region-based voxel-wise correction (RBV, $n = 4$). The most frequently used region-based method was the geometric transfer matrix (GTM, $n = 4$). Malpetti et al. (2023) applied both IY and GTM correction methods for voxel-wise and region of interest (ROI) analysis respectively.

A large proportion of studies (94.74%) that conducted direct statistical group comparisons ($n = 19$) reported decreased synaptic density in one or more brain areas among individuals with neurodegenerative disorders compared to healthy controls (HC, $n = 18$, Fig. 2**A**). Furthermore, most studies (73.33%) that inquired into the relation between synaptic density and cognitive functioning ($n = 15$) reported associations between synaptic loss and global or domain-specific cognitive decline ($n = 11$, Fig. 2**B**). These significant correlations were evident in studies focusing on AD and aMCI ($n = 6$), Frontotemporal lobar degeneration pathologies (FTLD, $n = 4$), and Lewy body diseases ($n = 1$). See supplemental materials for a detailed visualisation of these results (Fig. S3).

4. Discussion

The primary objective of this systematic review was to offer a thorough summary of current research on *in vivo* SV2A PET imaging in neurodegenerative disorders. Discussing the novel and rapidly developing area of *in vivo* SV2A PET imaging, we begin by reviewing the outcomes of validation studies. Afterwards, we address synaptic density in the context of normal ageing and extend our scope by encompassing its manifestations in various neurodegenerative disorders: aMCI, AD, FTLD pathologies, Lewy body diseases, HD, and SCA3. Following this, the relation of in vivo synaptic density loss to cognitive decline, as well as other markers of pathologies is explored.

Table 1
Characteristics and principal findings from included clinical studies.

Authors	If reported or calculable from data. Disease state (amyloid positivity): size, sample breakdown (x/x). Follow-up time point (months ± SD)	Mean age ± SD, gender breakdown (m:f)	Imaging modality and acquisition (radioligand: reference region)	Principal findings
(Chen et al., 2018)	AD/aMCI (9 Aβ+): n = 10 (5/5) HC (10 Aβ-): n = 11	72.7 ± 6.3, 5:5 72.9 ± 8.7, 5:6	Dynamic PET ([^{11}C]UCB-J: SO, [^{11}C]PiB: CBL) T1 MRI (3 T)	• Regional reduction of [^{11}C]UCB-J binding in HIP of AD. • Reduced HIP [^{11}C]UCB-J binding related to global cognitive decline and composite episodic memory score.
(Bastin et al., 2020)[a]	AD/aMCI (Aβ+): n = 25 (19/6) HC (8 Aβ-): n = 21	73.3 ± 8.0, 11:14 71.5 ± 4.5, 11:10	Dynamic PET ([^{18}F]UCB-H: IDIF, [^{18}F]-FDG: pons) T1 MRI (3 T)	• Prominent reduction of synaptic density in right anterior HIP extending to entorhinal cortex of AD/aMCI. • Reduced regional [^{18}F]UCB-H distribution in HIP related to anosognosia for memory and global cognitive decline, but not related to hypometabolism measured earlier.
(Chen et al., 2021)	AD/aMCI (Aβ+): n = 14 (4/10) HC (Aβ-): n = 11	69.6 ± 5.7, 7:7 69.4 ± 9.0, 3:8	Dynamic PET ([^{11}C]UCB-J, [^{18}F]FDG: CBL) T1 MRI (field strength not reported)	• Similar loss of [^{11}C]UCB-J binding and hypometabolism in medial temporal regions in AD compared to HC. • Smaller magnitude of [^{11}C]UCB-J reduction than [^{18}F]FDG in neocortical regions.
(Coomans et al., 2021)	AD (Aβ+): n = 7	64.3 ± 8.2, 4:3	Dynamic PET-CT ([^{18}C]UCB-J: SO, [^{18}F]flortaucipir: GM CBL) MEG T1 MRI (3 T)	• [^{18}F]flortaucipir uptake inversely related to [^{11}C]UCB-J uptake, particularly in AD patients with substantial neocortical tau pathology levels. • Higher regional [^{18}F]flortaucipir and reduced regional [^{11}C]UCB-J binding associated with altered synaptic functioning, most pronounced in OccL. • [^{18}F]flortaucipir but not [^{11}C]UCB-J, binding related to global cognitive decline.
(Mecca et al., 2022)	AD/aMCI (Aβ+): n = 10 (5/5) HC (Aβ-): n = 10	68.8 ± 6.6, 4:6 72.1 ± 7.9, 4:6	Dynamic PET ([^{11}C]UCB-J: CBL, [^{18}F]flortaucipir: inferior GM CBL, [^{11}C]PiB: CBL) T1 MRI (3 T)	• Lower [^{11}C]UCB-J binding in HIP of AD. • ERC [^{18}F]flortaucipir uptake inversely related to [^{11}C]UCB-J binding in HIP across groups, but not in HC and AD/aMCI groups individually.
(Mecca, O'Dell et al., 2022)	AD/aMCI (Aβ+, early): n = 45 (28/17) HC (Aβ-): n = 19	70.82 ± 7.48, 23:22 70.84 ± 7.78, 9:10	Dynamic PET ([^{11}C]UCB-J, [^{11}C]PiB: SO and CBL) T1 MRI (field strength not reported)	• Global [^{11}C]UCB-J binding in AD-affected regions related to global and domain-specific cognitive functioning in AD/aMCI. • Global [^{11}C]UCB-J binding is a stronger predictor of cognitive functioning than GM volume.
(Vanderlinden et al., 2022)[b]	BL aMCI (11 Aβ+): n = 12 HC (4 Aβ+): n = 26 Follow up (25.0 ± 1.3) aMCI: n = 12	BL 71.6 ± 5.3, 6:6 68.9 ± 9.1, 14:12 Follow up -	Static PET-MR ([^{11}C]UCB-J: SO, [^{18}F]MK6240: Inferior CBL) PET-CT ([^{11}C]PiB) T1 MRI (3 T)	• Regional decrease in [^{11}C]UCB-J binding in the mesotemporal cortex of aMCI at baseline, extending to widespread synaptic density loss at follow-up. • Baseline global [^{18}F]MK6240 binding inversely related to^{11}C-UCB-J binding at follow-up in aMCI. • Baseline^{11}C-UCB-J binding in MTL related to global cognitive functioning. • Longitudinal change in MTL^{11}C-UCB-J binding related to episodic memory, but not to other domain-specific cognitive functions or global cognition.
(Venkataraman et al., 2022)	BL AD (Aβ+): n = 12 HC: n = 16 Follow up (14.27 ± -) AD (Aβ+): n = 8	BL 75.50 ± 7.82, 6:6 65.88 ± 9.82, 8:8 Follow up -	Dynamic PET-CT ([^{11}C]SA-4503, [^{18}F]BCPP-EF, [^{11}C]UCB-J: SO) T1 MRI (3 T)	• Regional decreased [^{11}C]UCB-J binding in AD, most pronounced in Cau, HIP, and THA. • Loss of normal physiological relationship between mitochondrial oxidative phosphorylation and synaptic density in AD. • Regional [^{11}C]UCB-J binding in HIP and parietal lobe strongly related to language functions. • No longitudinal changes in regional [^{11}C]UCB-J binding.
(Zhang et al., 2023)	AD: n = 33 (Aβ+) aMCI: n = 31 (Aβ+) HC: n = 30	68.0 ± 7.8, 14:19 70.1 ± 6.8, 13:18 63.4 ± 8.0, 6:24	Static PET-MR ([^{18}F]SynVesT-1: CBL) T1 MRI (3 T), diffusion MRI, resting state fMRI.	• Lower [^{18}F]SynVesT-1 binding in cortical and hippocampal areas in AD, but not aMCI. • Synaptic density in the right insular cortex, bilateral MFG and right hippocampus related to global cognitive functioning in AD/MCI. • Reduced^{18}F]SynVesT-1 binding in MFG linked to functional and structural connectivity alterations with SFG region.
(Holland et al., 2020)	PSP: n = 14 CBS (9 Aβ-): n = 15 HC: n = 15	72.79 ± 7.74, 7:7 70.56 ± 8.23, 7:2 68.0 ± 7.45, 7:8	Dynamic PET-MR ([^{11}C]PiB: CBL, [^{11}C]UCB-J: SO) T1 MRI (3 T)	• Widespread (sub)cortical reductions of [^{11}C]UCB-J binding, also in non-atrophied areas. • Global [^{11}C]UCB-J binding was inversely related to PSP and CBS disease severity and directly related to global cognitive functioning.

(*continued on next page*)

Table 1 (*continued*)

Authors	If reported or calculable from data. Disease state (amyloid positivity): size, sample breakdown (x/x). Follow-up time point (months ± SD)	Mean age ± SD, gender breakdown (m:f)	Imaging modality and acquisition (radioligand: reference region)	Principal findings
(Mak et al., 2021)	PSP: n = 22 CBS (Aβ-): n = 14 HC: n = 27	70.9 ± 8.69, 10:12 70.0 ± 7.91, 9:5 69.0 ± 7.34, 16:11	Dynamic PET-MR ([^{11}C]PiB: CBL, [^{11}C]UCB-J: SO) T1 MRI (3 T), diffusion MRI	• Extensive and severe reductions of [^{11}C]UCB-J binding across (sub)cortical regions in PSP and CBS, also in non-atrophied areas. • Stronger [^{11}C]UCB-J binding reduction effects across whole brain compared to ODI and GM atrophy.
(Salmon et al., 2021)[c]	bvFTD (mild to moderate): n = 12 HC: n = 12	73.5 ± 7.6, 8:4 71.4 ± 5.2, 7:5	Dynamic PET ([^{18}F]UCB-H: IDIF) T1, MRI (3 T)	• Regional [^{11}C]UCB-J binding reduction related to loss of dendritic complexity in PSP/CBS. • Decreased [^{18}F]UCB-H distribution in anterior parahippocampal gyrus in bvFTD (trend level). • Anosognosia for clinical symptoms inversely related to [^{18}F]UCB-H distribution in right Cau head of bvFTD.
(Holland et al., 2022)	PSP: n = 23 CBS (Aβ-): n = 12 HC: n = 19	71.3 ± 8.6, 10:13 70.9 ± 7.9, 7:5 68.9 ± 7.1, 11:8	Dynamic PET-MR ([^{11}C]PiB: CBL, [^{18}F]AV-1451: inferior CBL, [^{11}C]UCB-J: SO) T1 MRI (3 T)	• Reduced regional [^{11}C]UCB-J binding across all (sub) cortical areas in PSP/CBS. • [^{11}C]UCB-J binding directly related to [^{18}F]AV-1451 binding, but less so in individuals with higher disease severity. • Cortical [^{18}F]AV-1451 binding inversely related to subcortical [^{11}C]UCB-J binding.
(Holland et al., 2023)	BL PSP: n = 32 CBS (Aβ-): n = 16 HC: n = 31 Follow up PSP: n = 16 (13.8 ± 5.5) CBS (Aβ-): n = 6 (12.0 ± 4.3)	BL - - 71.0 ± 8.5, 20:11 Follow up 72.1 ± 8.1, 7:9 71 ± 10.8, 2:4	Dynamic PET-MR ([^{11}C]PiB: CBL, [^{11}C]UCB-J: SO) T1 MRI (3 T)	• Widespread loss of [^{11}C]UCB-J binding across all (sub)cortical areas in PSP/CBS. • Regional longitudinal loss of [^{11}C]UCB-J binding within frontal lobe and right caudate in PSP/CBS. • Longitudinal loss off [^{11}C]UCB-J binding in frontal lobe related to cognitive functioning. • Faster reductions in frontal [^{11}C]UCB-J binding associated with faster cognitive functioning.
(Malpetti et al., 2023)	bvFTD: n = 11 HC: n = 25	65.7 ± 9.3, 9:2 70.2 ± 7.0, 16:9	Dynamic PET-MR ([^{11}C]UCB-J: SO) T1 MRI (3 T)	• Global and regional mild to severe loss of [^{11}C]UCB-J binding in bvFTD, most pronounced in frontal, temporal, and cingulate cortex. • Synaptic density in frontal and cingulate regions related to cognitive performance. • Pattern of synaptic loss more extensive than GM atrophy.
(Matuskey et al., 2020)	PD: n = 12 (moderate to severe) HC: n = 12	61 ± 10, 4:8 60 ± 9, 4:8	Dynamic PET ([^{11}C]UCB-J: SO) T1 MRI (3 T)	• Lower [^{11}C]UCB-J binding in primary and secondary PD-related brain regions. • [^{11}C]UCB-J binding not related to neurocognitive functioning.
(Wilson et al., 2020)	BL (very early drug-naïve) PD: n = 12 HC: n = 16 Follow up PD: n = 9	BL 59.8 ± 9.0, 6:6 61 ± 12.5, 8:8 Follow up 59.2 ± 9.7	Dynamic PET-CT ([^{11}C]UCB-J: SO, [^{11}C]SA-4503, [^{18}F]BCPP-EF) T1 MRI (3 T)	• Reduced cross-sectional, but not longitudinal, [^{11}C]UCB-J distribution in primary PD-related regions in early symptomatic stages of PD. • Reduced [^{11}C]UCB-J distribution in BST related to motor symptom severity. • Colocalised loss of [^{11}C]UCB-J, [^{11}C]SA-4503, and [^{18}F]BCPP-EF.
(Delva, Van Laere et al., 2022)[d]	BL (early) PD: n = 30 HC: n = 20 Follow up PD: n = 27 (26.8 ± 2.0) HC: n = 18 (26.1 ± 2.3)	BL 60.4 ± 9.7, 19:8 59.3 ± 8.6, 13:5 Follow up 62.7 ± 9.8, 19:8 61.3 ± 8.6, 13:5	Static PET-MR ([^{18}F]FE-PE2I: OCX) Static PET-CT ([^{11}C]UCB-J: SO) MRI (field strength not reported)	• Lower [^{11}C]UCB-J binding in SN of PD at BL and follow-up, as well as in dorsal striatum, CAU, and PUT (trend level). • No regional longitudinal changes in [^{11}C]UCB-J binding in PD. • Global and regional [^{11}C]UCB-J binding not related to neurocognitive functioning, despite deteriorations in motor symptoms.
(Andersen et al., 2023)[e]	nPD: n = 21 DLB/PDD: n = 13 (9/4) HC: n = 15	(71.7 ± 6.4), 12:9 (74.3 ± 4.7), 12:1 (72.4 ± 4.2), 8:7	Dynamic PET-CT ([^{11}C]UCB-J, [^{18}F]FDG: SO) T1 and T2 MRI (3 T)	• Regional loss of [^{11}C]UCB-J binding in DLB/PDD, but not nPD. • Minor global reduction in [^{11}C]UCB-J binding in DLB/PDD. • Smaller magnitude and spatial extent of [^{11}C]UCB-J reduction than [^{18}F]FDG in DLB/PDD. • Weak correlations between [^{11}C]UCB-J binding and domain-specific neurocognitive functioning in DLB/PDD.
(Delva, Michiels et al., 2022)	HD premanifest/early manifest: n = 18 (7/11) HC: n = 15	51.4 ± 11.6, 12:6 52.3 ± 3.5, 11:4	Static PET-CT ([^{11}C]UCB-J: SO) PET-MR ([^{18}F]FDG: pons) T1 MRI (3 T)	• More widespread reduction of [^{11}C]UCB-J binding in early manifest compared to premanifest HD. • Binding reduction [^{11}C]UCB-J more extensive than [^{18}F]FDG. • [^{11}C]UCB-J binding related to glucose metabolism in PUT and Cau across patients.

(*continued on next page*)

Table 1 (*continued*)

Authors	If reported or calculable from data. Disease state (amyloid positivity): size, sample breakdown (x/x). Follow-up time point (months ± SD)	Mean age ± SD, gender breakdown (m:f)	Imaging modality and acquisition (radioligand: reference region)	Principal findings
(Chen et al., 2023)[f]	SCA3 preataxic: n = 16 SCA3 ataxic: n = 27 HC: n = 22	34 ± 6.79, 10:6 43 ± 8.49, 13:14 33.5 ± 10.68, 8:14	Static PET-CT ([^{18}F] SynVesT-1: SO) T1 MRI (field strength not reported, only cohort 1)	• [^{11}C]UCB-J binding in PUT related to motor symptom severity across patients. • Global and regional [^{18}F]SynVesT-1 binding reductions. • Loss of [^{18}F]SynVesT-1 binding more widespread in ataxic compared to preataxic SCA3 and HC, and most pronounced in vermis, CBL and BST regions. • Preataxic and ataxic SCA3 individuals distinguishable based on regional synaptic density. • Regional synaptic density inversely related to disease severity.

Notes: [a] Fifteen Aβ-positive patients $n = 15$ (11 AD / 4 aMCI) underwent a [^{18}F]FDG PET scan earlier (23.8 months ± 12.7); [b] This study is a continuation of Vanhaute et al. (2020); [c] Healthy controls were selected from a previously published study by Bastin et al. (2020); [d] Baseline results of this longitudinal study were published in Delva et al. (2020); [e] Baseline results of this longitudinal study were published in Andersen et al. (2021); [f] A second cohort of SCA3 patients ($n = 31$, 7 preataxic / 24 ataxic) received a simplified PET procedure for validation of clinical application. The results obtained from this group are not provided in the table. A*bbreviations:* - = not reported; AD = Alzheimer's disease; aMCI = amnestic Mild Cognitive Impairment; Aβ- = Amyloid-β negative; Aβ+ = Amyloid-β positive; BL = Baseline; BST = Brainstem; bvFTD = Frontotemporal dementia, behavioural variant; Cau = Caudate; CBL = Cerebellum; CBS = Corticobasal syndrome; DLB = Dementia with Lewy bodies; ERC = Entorhinal cortex; fMRI = functional-(MRI)*;* GM = Grey matter; HC = Healthy controls; HD = Huntington's disease; HIP = Hippocampus; IDIF = Image-derived input function; MEG = Magnetoencephalography*;* MFG = Middle frontal gyrus; MRI = Magnetic Resonance Imaging; MTL = Medial temporal lobe*;* nPD = Non-demented Parkinson's disease; OccL = Occipital lobe; OCX = Occipital cortex; ODI = Orientation Dispersion Index*;* PD = Parkinson's disease; PDD = Parkinson's disease with dementia; PET = Positron emission tomography; PET-CT = (PET)-Computerised Tomography*;* PET-MR = (PET)-Magnetic Resonance*;* PSP = Progressive supranuclear palsy; PUT = Putamen; SCA3 = Spinocerebellar Ataxia Type 3; SFG = Superior frontal gyrus; SN = Substantia nigra; SO = Centrum semi-ovale; THA = Thalamus.

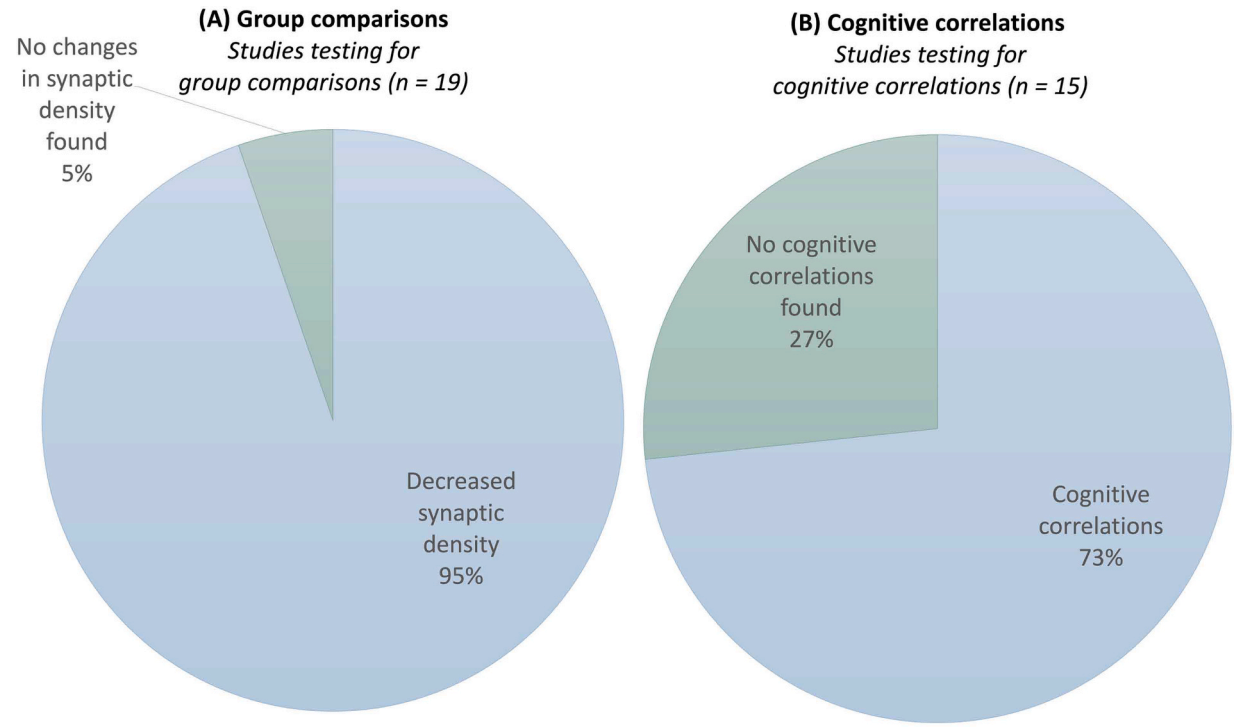

Fig. 2. Percentage of clinical studies showing group differences in synaptic density and correlations with cognitive functioning **(filename = Fig. 2.colourised_M. Visser)** *Notes.* "Decreased synaptic density" indicates the presence of statistically significant group differences (adjusted for multiple comparisons) in one or more brain regions between diseased subjects and controls. Longitudinal studies were included if they identified cross-sectional differences at baseline, follow-up, or both. "Cognitive correlations" indicate statistically significant associations (adjusted for multiple comparisons) between synaptic density in one or more brain regions and neuropsychological tests measuring global or domain-specific cognitive functioning in diseased subjects, excluding motor functioning. Longitudinal studies were included if associations between changes in synaptic density over time and cognitive performance were found.

4.1. Validation studies

4.1.1. Tracer kinetic modelling

A range of kinetic models have been investigated to identify the optimal kinetic analysis model for *in vivo* SV2A PET. In current literature, full kinetic modelling with arterial blood sampling confirmed the 1-Tissue-Compartment (1TC) model as most suitable to describe cerebral [^{11}C]UCB-J and [^{18}F]SynVesT-1 tracer kinetics (Finnema et al., 2018; Koole et al., 2019; Li et al., 2021; Tuncel et al., 2021). Given the strong correlation between the Multilinear Analysis 1 (MA1) and

1TC-derived V_T estimates, MA1 may also be considered appropriate (Mansur et al., 2020; Naganawa et al., 2021). Furthermore, in various studies, Akaike Information Criterion and F-test preferred the 2-Tissue--Compartment (2TC) model over 1TC, however, the 2TC faced challenges in reliably estimating kinetic parameters (Mansur et al., 2020; Naganawa et al., 2021; Tuncel et al., 2021). Results were inconclusive regarding the additional inclusion of a blood volume fraction as a parameter (1T2k_V_B) into this kinetic evaluation. Finnema et al. (2018) reported 1T2k_V_B inclusion did not affect regional V_T values, causing Rossano et al. (2020) to obtain from using it. Others did include the 1T2k_V_B metric (Koole et al., 2019; Mansur et al., 2020; Tuncel et al., 2021), with Tuncel et al. (2021) and Mansur et al. (2020) suggesting it enhances the description of [^{11}C]UCB-J kinetics.

4.1.2. Reference tissue modelling

To make PET radioligands more suitable for clinical use, the preference lies in utilising practical, non-invasive alternative approaches to arterial blood sampling. One approach is the use of reference tissue models, which allow for the quantification of BP_{ND} (Zanderigo et al., 2013). Various studies have validated different parametric methods for quantifying SV2A binding using subcortical white matter (WM) as reference tissue (i.e., centrum semi-ovale; SO). These included the Simplified Reference Tissue Model (SRTM), static SUVR, Multilinear Reference Tissue Model (MRTM), and reference Logan Graphical Analysis (rLGA). Across studies, the $SRTM2_{SO}$ was considered the most appropriate choice for [^{11}C]UCB-J quantification. STRM2 corresponds best to plasma input-derived DVR, although signal underestimation was observed (Koole et al., 2019; Mertens et al., 2020; Tuncel et al., 2021; Tuncel et al., 2022). Additionally, a $SUVR_{SO}$ approach was also identified as a valuable alternative for full kinetic modelling or STRM, particularly since the precision of the latter decreases when scanning time is < 60 min, limiting clinical applicability (Koole et al., 2019; Mertens et al., 2020).

4.1.3. Reference tissue selection

The SO has been validated as a reference region for the quantification of SV2A density. Comparing baseline and post-SV2A-drug (Padsevonil) scanning [^{11}C]UCB-J, no significant changes in the SO distribution volume (1TC-derived) were identified. Meanwhile, regional V_T values were significantly reduced in other regions, suggesting negligible target expression in the SO (Koole et al., 2019). Further supporting its potential as reference tissue, Mansur et al. (2020) demonstrated [^{11}C]UCB-J V_T estimates to be approximately 60% lower in the SO. Tuncel et al. (2021) additionally found no significant difference in SO V_T's between AD patients and HC.

Ideally, there should be no specific or displaceable tracer uptake in a reference region. In response to Finnema et al. (2016), who indicated the presence of displaceable activity in the SO, Rossano et al. (2020) further carefully characterised SO [^{11}C]UCB-J binding. Even when they minimised the effects of GM matter spill-in, partial volume, and low-intensity WM biases, displaceable SO [^{11}C]UCB-J uptake was not fully eliminated. In particular, SO V_T overestimates GM V_{ND} uptake. Consequently, BP_{ND} is negatively biased if SO is used as a reference. Nevertheless, SO V_T and GM V_{ND} estimates are highly intercorrelated and potential differences in [^{11}C]UCB-J behaviour between GM and WM tissue types may be consistent within and between groups (Rossano et al., 2020; Tuncel et al., 2022). Therefore, the SO region is still thought to be a suitable reference region for [^{11}C]UCB-J.

The current review did not include studies validating the use of a cerebellar (CBL) reference region, as these were excluded due to overlapping samples with more recent publications (see Table S3). Nonetheless, given its relevance, validation of conversion from SO to CBL reference regions in [^{11}C]UCB-J PET, as conducted by Mecca et al. (2020) and O'Dell et al. (2021), will be addressed briefly. Overall, values of DVR_{CBL} demonstrated notably lower variability than DVR_{CS} and showed a comparable level of correlation with DVR values obtained using the 1TC model and metabolite-corrected arterial plasma curves (Mecca et al., 2020; O'Dell et al., 2021). More validation studies assessing the potential of CBL as a reference region are warranted.

4.1.4. Test-retest reliability

For [^{11}C]UCB-J V_T, absolute test–retest (TRT) reproducibility ranges between 3–9% across regions in healthy subjects, which is exceptionally good compared to TRT of other tracers previously reported (Finnema et al., 2018). In AD patients, a mean 28-day TRT of $< 15\%$ was identified for V_T, plasma input-derived DVR and SRTM BP_{ND}. This suggests that [^{11}C]UCB-J can be used to quantify the effect of therapeutical interventions on SV2A if the effect size of the intervention is higher than 15% (Tuncel et al., 2021). Tuncel et al. (2022) further evaluated TRT for whole-brain analysis and found that reproducibility was much better for HC compared to patients with AD. However, larger TRT variability in patients is to be expected given synaptic density reductions depend on disease severity and GM atrophy, which may vary per individual (Tuncel et al., 2022). In comparison to [^{11}C]UCB-J, absolute TRT reproducibility for [^{18}F]SynVesT-1 (performed 7 ± 7 days apart) was similar for V_T and slightly less for BP_{ND} across regions, with values of $< 9\%$ (Li et al., 2021). Overall, both same-day and 28-day TRT reproducibility of [^{11}C]UCB-J and [^{18}F]SynVesT-1 V_T and BP_{ND} are found to be excellent (Finnema et al., 2018; Li et al., 2021; Tuncel et al., 2021; Tuncel et al., 2022).

4.2. Synaptic density in cognitively normal individuals

4.2.1. Preservation of synaptic density during healthy ageing

Accurate interpretation of *in vivo* SV2A PET imaging studies in dementia necessitates careful consideration of synaptic density in healthy individuals as well as the potential impact of demographic factors. Michiels et al. (2021) were the first to investigate the effects of ageing and sex on [^{11}C]UCB-J binding *in vivo*. Their study of 78 cognitively normal subjects aged 18–85 years revealed remarkable stability of synaptic density with advancing age, except for a slight reduction in the caudate nucleus (1.7% per decade), possibly linked to ventricle enlargement. Additionally, no substantial sex-based differences in synaptic density or age-sex interaction were observed (Michiels et al., 2021). Andersen et al. (2022) expanded upon these findings with a study involving 26 healthy subjects divided into two age groups (20–30 and 65–85). In addition to assessing synaptic density using [^{11}C]UCB-J, cerebral metabolism was examined using [^{18}F]FDG. Results reaffirmed the findings of Michiels et al. (2021), providing further evidence that, although synaptic loss contributes to the overall loss of GM volume during ageing, the density of the synapses per volume of GM integrity remains preserved in the healthy ageing brain. In other words, volume loss is proportional to synaptic loss with ageing, resulting in stable synaptic density (Andersen et al., 2022). Additionally, a widespread reduction of [^{18}F]FDG uptake in the older age group was observed, aligning with the findings of numerous other studies (Chetelat et al., 2013; Fujimoto et al., 2008; Hsieh et al., 2012; Yoshizawa et al., 2014). Moreover, regional differences in relative [^{18}F]FDG vs. [^{11}C]UCB-J uptake were identified, suggesting "some synapses are on average more hungry than others", given their higher relative metabolic demands (Andersen et al., 2022, p. 56). These findings align with an earlier multi-tracer study by van Aalst et al. (2021) in 20 young healthy female subjects. Both studies observed higher relative [^{11}C]UCB-J uptake in the temporal lobe and higher relative [^{18}F]FDG uptake in frontal areas (Andersen et al., 2022; van Aalst et al., 2021). There thus seems to exist a spatially variant decoupling of relative synaptic density and metabolic activity in healthy individuals. Interestingly, this relationship may be slightly affected by age, especially in the frontal lobe, where lower glucose consumption per synapse was observed in the older group (2%) compared to the younger group (5%). However, the limited sample size in Andersen et al.'s (2022) study cautions against making definitive conclusions from this discovery. Overall, studies collectively support the

notion that synaptic density remains relatively preserved during healthy ageing, despite age-related changes in cerebral metabolism and grey matter volume.

4.2.2. Exploring the relationship between synaptic density and resting-state network functioning

Synaptic density has not only been linked to local synaptic activity, but also to the healthy brain's functional organisation, that is, resting-state network (RSN) activity (Fang et al., 2021; Fang et al., 2023). Fang et al. (2021) applied independent component analysis (ICA) to [^{11}C]UCB-J V_T data and reliably extracted multiple source-based patterns (i.e., networks) of coherent synaptic density variability. Based on visual comparison, Fang and colleagues argue that the spatial organisation of synaptic density network variability shows some similarity with that of canonical RSNs, but appears to be more consistent with GM and glucose metabolism (Fang et al., 2021). Subsequently, in their 2023 study, (Fang et al.) conducted a quantitative investigated into this relationship. A robust correlation was identified between functional amplitudes in the anterior default-mode network and networks of synaptic density that are both anatomically connected (e.g., the medial prefrontal cortex), and functionally associated (e.g., the striatum). Contrary to expectations, no other strong relations were found between networks of synaptic density and spatially overlapping or functionally associated RSNs of interest, implying the degree to which synaptic density underlies RSN amplitudes is multifactorial and requires further investigation (Fang et al., 2021; Fang et al., 2023).

4.3. Application of SV2A PET imaging in the investigation of neurodegenerative disorders

4.3.1. Pairwise comparisons

4.3.1.1. Alzheimer's disease. Chen et al. (2018) were the first to study *in vivo* SV2A PET in AD and aMCI. They demonstrated lower [^{11}C]UCB-J BP_{ND} in the hippocampus (−41%) of 9 mild AD/aMCI patients compared to 11 HC ($SRTM2_{SO}$-derived). Exploratory voxel-wise analysis suggested an additional significant binding reduction in the entorhinal cortex; however, this result was uncorrected for multiplicity and did not withstand PVC. In a larger sample size, using an SV2A radiotracer with a longer half-life ([^{18}F]UCB-H; $T_{1/2}$ = 110 min), Bastin et al. (2020) confirmed the findings of Chen et al. (2018) and revealed significant synaptic density reduction (V_T) in the right anterior hippocampus (−26.9%) in AD/aMCI patients, which extended to the entorhinal cortex. Subsequently, based on earlier studies by Mecca et al. (2020) and O'Dell et al. (2021) -not included in the current review due to overlapping samples-, Chen et al. (2021) adjusted their methodology. When regional distribution volume ratios were computed using the cerebellum as an alternative reference region, widespread synaptic density loss was observed in medial temporal and thalamic regions, as well as some small between-group differences in susceptible neocortical regions (−7.6% to −24.8%, Chen et al., 2021). In a related study, Mecca, Chen et al. (2022) reported reduced hippocampal [^{11}C]UCB-J binding (DVR_{CBL}) in AD/aMCI, but were unable to statistically confirm group differences. This null-finding might be attributed to the fact that Chen et al. (2021) directly derived DVRs for the ROIs from 1TC parameters using AIF, rather than using the reference-region-based analysis employed by Mecca, Chen et al. (2022). Furthermore, in aMCI exclusively, cross-sectional evaluation at baseline and follow-up revealed a significant decrease in SV2A binding in the mesotemporal cortex, which had progressed to the entire mesotemporal, inferior frontal, precuneus and temporo-occipital secondary cortex two years later (Vanderlinden et al., 2022). In AD patients, Venkataraman et al. (2022) also demonstrated a focal AD-related decrease in synaptic binding, largest in the caudate (−25%), hippocampus (−24%), and thalamus (−19%). Most recently, a larger cohort study utilising a difluoro-analogue of UCB-J, reported reduced binding of [^{18}F]SynVesT-1 in the hippocampus and bilateral cortex of AD patients. In comparison to aMCI, AD patients showed reduced synaptic density in the middle frontal gyrus and right insular cortex (Zhang et al., 2023). Together, these findings indicate the medial temporal lobe is the most robust site of synaptic density loss across the continuum of AD, evident across a diverse range of methodologies and radiotracers. Evidence for reduced synaptic density in association cortices is somewhat inconsistent, possibly due to limited statistical power and the inclusion of predominantly early-stage AD patients.

4.3.1.2. Frontotemporal lobar degeneration pathologies. Initial *in vivo* evidence of synaptic loss in FTLD pathologies came indirectly through a case report by Malpetti et al. (2021) on risk-gene carriers. Subsequently, Salmon et al. (2021) conducted the first exploratory research in 12 bvFTD (i.e., behavioural variant) and 12 HC participants. A trend-level reduction of [^{18}F]UCB-H V_T in the right parahippocampal region (−41%) in bvFTD compared to HC was reported, but no frontal synaptic loss or difference between bvFTD and AD was identified (Salmon et al., 2021). A subsequent study employed a radiotracer with higher specific binding, a kinetic analysis with more sensitivity to synaptic changes ([^{11}C]UCB-J BP_{ND}), as well as a sample comprising patients with longer symptom duration and lower cognitive performance (Malpetti et al., 2023). Reportedly, synaptic loss was severe, with binding reduction being most pronounced in frontotemporal, insular, and cingulate regions. Moreover, the effect sizes and regional extent of disease-related synaptic density loss were notably larger than those of GM atrophy (Malpetti et al., 2023). In PSP and CBS, a similar pattern was observed, with synaptic density demonstrating a more pronounced and widespread degree of reduction compared to the extent of GM atrophy (Holland et al., 2023; Holland et al., 2020; Holland et al., 2022; Mak et al., 2021). It is worth noting that PSP/CBS studies were conducted using a highly similar methodology, allowing for more reliable and comparable results. In patient cohorts compared to HC, reduced [^{11}C]UCB-J BP_{ND} was consistently reported in all cortical lobes, as well as in the cingulate, hippocampus, insula, amygdala, and subcortical structures across studies. Severe synaptic density loss was observed in similar regions in both PSP and CBS (i.e., medulla and caudate nucleus), but also in distinct regions between the two conditions (no statistical testing). Overall, frontotemporal lobar degeneration pathologies are marked by widespread, severe synaptic density loss in both cortical and subcortical regions, including regions affected in later stages of disease and non-atrophied areas.

4.3.1.3. Lewy body diseases. Matuskey et al. (2020) provided the first evidence of synaptic loss in PD. In 12 moderate to advanced PD patients compared to 12 HC, reduced [^{11}C]UCB-J BP_{ND} was reported in PD-related brainstem nuclei, particularly in the substantia nigra (SN, −45%), red nucleus (−31%), locus coeruleus (−17%), as well as in some cortical areas, such as the parahippocampal gyrus (−12%). In a pilot study with 12 very early drug-naive PD patients, Wilson et al. (2020) corroborated this finding and observed reduced lower synaptic density ([^{11}C]UCB-J V_T) in primary PD-related brain regions as well, although less pronounced in the SN (−7%). Note that effects of tissue atrophy could not be ruled out as no PVC was performed (Wilson et al., 2020). A larger cohort of 27 early PD and 18 HC participants showed [^{11}C]UCB-J was significant in the SN (−15%), consistent with baseline results (Delva et al., 2020), and at trend-level in striatal areas (−6% to −7%, Delva, Van Laere et al., 2022). Furthermore, in a mixed sample of patients with PD and dementia (PDD) and DLB, Andersen et al. (2023) demonstrated clear reductions in synaptic density, as measured with [^{11}C]UCB-J SUVR-1, across most cortical regions (−21% to −46%). Collectively, these findings suggest that synaptic density loss occurs early in the pathophysiology of PD, beginning in PD-related brainstem nuclei like the substantia nigra, and extending to the cortex in more advanced stages that come with cognitive impairment.

4.3.1.4. Other neurodegenerative disorders. At present, Delva, Michiels et al. (2022) is the only study providing *in vivo* evidence of early, multifocal, synaptic density loss in HD with [^{11}C]UCB-J PET (Rub et al., 2016; Vonsattel et al., 2011). HD is caused by CAG expansion in the *IT15* gene, leading to the production of a polyglutamine (polyQ) stretch in the huntingtin protein. In premanifest HD, synaptic loss was identified in putamen (−19%) and caudate (−16%) only. As for early manifest HD, further extra striatal decreases in SV2A binding were observed in the pallidum (−30%), as well as cortically (−11% to −12%). Unexpectedly, SV2A loss in the cerebellum (−14%) was discovered, providing support for cerebellar involvement in the early stages of symptomatic HD (Delva, Michiels et al., 2022). Recently, an SV2A PET study was conducted on another polyQ-related disorder, namely Spinocerebellar ataxia (Machado-Joseph disease; SCA3, Chen et al., 2023). SCA3 is instigated by CAG repeat expansion in the *ATXN3*, encoding for a polyQ stretch in the ataxin-3 protein. Compared to HC, preataxic SCA3 patients exhibited [^{18}F]SynVesT-1 SUVR reductions only in the vermis (−6%). In ataxic SCA3 patients, more significant synaptic loss was observed in the vermis (−16%), extending to extra-cerebellar regions, encompassing the brainstem, caudate, putamen, and occipital lobe (−8% to −12%). Collectively, HD and SCA3 studies indicate significant reductions in synaptic density, evident even in the absence of severe symptoms, with HD showing pronounced loss in the striatum and SCA3 demonstrating reduction specifically in the vermis.

4.3.2. Longitudinal SV2A PET imaging in (pre)clinical dementia

To date, longitudinal research has been conducted in aMCI (Vanderlinden et al., 2022), AD (Venkataraman et al., 2022), PD (Delva, Van Laere et al., 2022; Wilson et al., 2020) and PSP and CBS (Holland et al., 2023). Although evidence for progressive *in vivo* synaptic loss is limited, variations in the pace of longitudinal decrease of synaptic density appear to exist across different neurodegenerative conditions. Along the Alzheimer's continuum, synapse density loss may show a more progressive pattern in patients at earlier stages of the disease spectrum. In aMCI patients exclusively, Vanderlinden et al. (2022), revealed longitudinal disparities in the left superior frontal cortex over a two-year follow-up period. Meanwhile, when solely investigating AD patients, no significant progressive loss in DVR_{SO} was identified 12 to 18 months later (Venkataraman et al., 2022). Note that Vanderlinden et al. (2022) used SUVR as the primary outcome measure, which is potentially biased due to changes in cerebral blood flow (CBF) and may be dependent on the extent of the underlying amyloid-β burden (Heeman et al., 2022). In comparison to AD, the rate of SV2A decline in early-stage PD appears to be relatively slow. In Wilson et al. (2020), 8 PD patients underwent a longitudinal [^{11}C]UCB-J PET scan at a 1-year interval with no significant changes detected. The caudate exhibited the most notable reduction in SV2A levels; however, this observation did not attain statistical significance (Wilson et al., 2020). A second study by Delva, Van Laere et al. (2022) attained a longer scan interval and larger sample size. Nevertheless, no [^{11}C]UCB-J SUVR-1 longitudinal changes were identified, suggesting synaptic density might not be a sensitive biomarker during the early phases of Lewy body diseases. The opposite seems to be true for PSP and CBS, providing promising results. Rapid longitudinal progression in [^{11}C]UCB-J BP_{ND} has been found in the frontal lobe (−3%), caudate nucleus (−4%), and left pallidum (−4%, trend level) after one year (Holland et al., 2023). Regardless, the consensus among these studies remains that further longitudinal investigations are necessary to ascertain whether SV2A PET possesses the capacity to serve as a clinical biomarker for monitoring the advancement of neurodegenerative disorders.

4.3.3. Synaptic density and cognitive functioning

Significant correlations were apparent between reduced synaptic density and overall cognitive decline in studies investigating patients with aMCI/AD (Bastin et al., 2020; Chen et al., 2018; Mecca, O'Dell et al., 2022; Zhang et al., 2023), FTLD (Holland et al., 2023; Holland et al., 2020), and DLB (Andersen et al., 2023). Generally, reported correlations were specific to disease-related regions, involving areas such as the hippocampus regions in aMCI/AD, as well as frontal and cingulate regions in FTLD pathologies. Notably, along the continuum of Alzheimer's disease, synaptic density is a significant predictor of cognitive performance across all domains, including language (Venkataraman et al., 2022), verbal and episodic memory (Bastin et al., 2020; Chen et al., 2018; Vanderlinden et al., 2022), and executive functioning, processing speed, and visuospatial ability (Mecca, O'Dell et al., 2022). In contrast, within Lewy body pathologies, the connection between synaptic density and domain-specific cognitive performance is notably weaker and limited. Such correlations were only observed within a specific subset of cases involving late-stage PD and DLB (Andersen et al., 2023). The exploration of whether synaptic density is associated with domain-specific cognition in the context of other neurodegenerative disorders remains an unexplored area.

Collectively, studies suggest synaptic density contributes significantly to cognitive impairment, and the application of SV2A PET imaging allows for precise mapping of behaviour and synaptic changes. Nevertheless, the extent to which synaptic density prevails over other metrics in predicting cognitive impairment remains uncertain, hinging on the pathological characteristics of each disease and their sequential progression. Notably, in cases where atrophy is minimal or absent, synaptic loss emerges as a critical mediator of cognitive decline (Malpetti et al., 2022; Mecca, O'Dell et al., 2022). Conversely, Coomans et al. (2021) report cognitive functioning to be more strongly associated with tau build-up instead of synaptic density. Presently, cognitive outcome measures seem to primarily serve exploratory purposes. There is a need for future studies on more in-depth neuropsychological assessments sensitive to subtle focal brain changes occurring in preclinical dementia (Ritchie et al., 2017).

4.3.4. Relation of in vivo synaptic density loss to other markers of pathologies

4.3.4.1. Synaptic density and hypometabolism. Several SV2A studies have employed [^{18}F]FDG to assess the relationship between synaptic density and reduced regional cerebral glucose consumption, indicative of impaired metabolic functionality (Dierckx et al., 2021). FDG PET detects not only cerebral hypometabolism but is also reputed to be an indirect measure of neuronal integrity (Carapelle et al., 2020). Consequently, alterations in synaptic density may lead to a decrease in cerebral energy requirements, and conversely, changes in energy demand might influence synaptic density. Exploratory analysis by Bastin et al. (2020) indicated an absence of correlation between AD-related loss of synaptic density in the hippocampus and posterior cingulate cortex and hypometabolism observed less than four years prior. This could be attributed to either a time-related progression in pathology or the capture of distinct pathological processes by the two radiotracers. Related studies acquired [^{18}F]UCB-H and [^{18}F]FDG PET imaging within a shorter period. In general, studies revealed positive correlations between hypometabolism and reduced synaptic density (Andersen et al., 2023; Chen et al., 2021; Delva, Michiels et al., 2022). Chen et al. (2021) and Andersen et al. (2023) both report a similar magnitude of reduced [^{11}C]UCB-J binding and [^{18}F]FDG metabolism in the medial temporal lobe. Moreover, the magnitude of hypometabolism was significantly greater relative to synaptic density loss in neocortical regions. Additionally, inter-tracer correlations in medial temporal regions were notably higher compared to neocortical regions (Andersen et al., 2023; Chen et al., 2021). Overall, this suggests a regional decoupling of synaptic density and metabolic activity may be present in both healthy (see Section 4.2) and neurodegenerative disease states. Nevertheless, the extent of cortical hypometabolism does not surpass synaptic loss in every neurodegenerative condition. Results of Delva, Michiels et al. (2022) suggest that in HD, cortical [^{11}C]UCB-J PET uptake is more

extensive, compared to [^{18}F]FDG uptake.

4.3.4.2. Synaptic density and tau. *In vivo* evidence indicating a link between tau pathology and synaptic density loss is prominent. Across subjects and ROIs, higher regional tau deposition, as measured with [^{18}F]flortaucipir and [^{18}F]MK-6240, is associated with reduced synaptic density (Coomans et al., 2021; Mecca et al., 2020; Vanderlinden et al., 2022). This relation is particularly apparent for subjects with substantial tau pathology in neocortical areas (Coomans et al., 2021), and found to be stronger compared to the inverse associations evident between regional tau and GM volume (Mecca et al., 2020). Furthermore, spatial overlap between higher [^{18}F]flortaucipir and lower [^{11}C]UCB-J binding is substantial (Coomans et al., 2021; Mecca et al., 2020). In line with the baseline study of Vanderlinden et al., 2022, (Vanhaute et al., 2020), the spatial pattern of tau burden seems to be slightly more widespread and pronounced compared to that of synaptic loss (Coomans et al., 2021). Additionally, a time delay between both biomarkers was found, suggesting the spatial progression of synaptic loss may follow that of tau pathology (Vanderlinden et al., 2022). In regions exhibiting elevated tau pathology, a decrease in synaptic density emerges with disease progression (Holland et al., 2022). Cumulatively, existing literature aligns with the hypothesis that tau is to precede and potentially drive the loss of synaptic function (Jack et al., 2018; Wu et al., 2021).

4.3.4.3. Synaptic density and other metrics. Instances of disease-related reduced uptake of [^{11}C]UCB-J have also been associated with less commonly employed metrics of pathology. For example, synaptic density loss has been linked to modified synaptic functionality, suggestive of slowing of oscillatory activity (Coomans et al., 2021), and impaired functional and related structural connectivity underlying cognitive impairment (Zhang et al., 2023). Furthermore, Mak et al. (2021) have revealed a tight coupling between synaptic density loss and altered postsynaptic dendritic density and complexity. This was quantified using the Neurite Density Index and the Orientation Dispersion Index (NODDI ODI), which is an emerging diffusion-weighted MRI-based biomarker to quantify the density of neurites and their orientational complexity (Mak et al., 2021; Zhang et al., 2012). The varied effects of synaptic density loss on neural activity, both in terms of functional communication and physical wiring, along with concurrent microstructural alterations collectively point to the complexity of the synaptic landscape. Further cross-validation of more advanced imaging markers with synaptic density is warranted.

4.4. Challenges to consider when interpreting SV2A PET imaging results

Here, we briefly discuss challenges posed by potential confounding factors and heterogeneity in study methodologies. Cerebral atrophic changes may lead to signal loss due to PVEs. A decrease in apparent radiotracer uptake may thus not exclusively indicate decreased synaptic density, but could also be influenced by a concurrent disease-related loss of GM tissue (Drzezga et al., 2014). To disentangle atrophy from SV2A loss, various PVC methods have been developed (for a review, see Erlandsson et al., 2012). Importantly, different PVC algorithms may lead to different conclusions, with IY providing a theoretically more accurate PVC method compared to MG (Lu et al., 2021). This review encompasses clinical studies using various PVC methods across neurodegenerative disorders. Methodological differences persist even among studies that concentrate on the same pathology. For instance, Matuskey et al. (2020), Delva, Van Laere et al. (2022), and Andersen et al. (2023) investigated synaptic density in Lewy body diseases, applying MG, RBV, and, GTM PVC approaches respectively. In addition, other potential sources of bias include inconsistencies in PET imaging modalities, radiotracer selection, and modelling approaches. Furthermore, while some studies excluded participants using medications with known affinity for SV2A (e.g., Donepezil or Levetiracetam, Holland et al., 2020; Malpetti et al., 2023; Matuskey et al., 2020; Vanderlinden et al., 2022; Venkataraman et al., 2022), in the remaining studies, either medication use was not reported in general, or methods to account for it were not implemented. Since it is unknown how other centrally acting therapeutics may alter SV2A and synaptic density, this could potentially influence study results. For instance, long-term Levodopa use appears to affect synaptic plasticity and may increase synaptic density through levodopa-induced dyskinesia (Calabresi et al., 2015; Hurley et al., 2005; Martin et al., 2023).

5. Summary, perspectives, and future directions

This systematic review provides an extensive synthesis of the current state of *in vivo* SV2A PET imaging research of neurodegenerative disorders. We have discussed the main findings concerning group differences and clinical-cognitive correlations and explored relations between SV2A PET and other markers of pathology.

In summary, PET imaging of SV2A directly measures synaptic vesicles and serves as a proxy for synaptic density, thereby contributing to our understanding of the pathological processes preceding atrophy in neurodegeneration. Qualified SV2A radiotracers are available and validation studies have successfully identified their optimal compartment models and parametric approaches. Synaptic density appears to remain relatively preserved in the healthy ageing population, which may imply that synaptic density loss observed in neurodegenerative disorders primarily stem from the progressive disease itself, rather than from the natural ageing process. While the reduction of SV2A expression may not be specific to neurodegeneration in general, abnormal synaptic changes were identified in a large majority of neurodegenerative disorders. The consensus regarding the direction of disease-related changes in synaptic density, despite methodological variation among studies, suggests a strong association across different neurodegenerative disorders. The regional and temporal patterns of these changes could potentially offer valuable information that may aid in distinguishing between neurodegenerative conditions. Numerous studies underscore strong group differences in which anatomical patterns of synaptic density loss are found to be specific to brain regions linked to respective diseases. Longitudinally, studies reveal variations in the pace of synaptic density decline, and signal change seems to correlate with disease progression overall. Furthermore, the multitude of correlations found between synaptic density and clinical-cognitive functioning signifies its role in cognitive impairment, both globally and within specific domains. The complex relationship between synaptic density loss and other molecular pathologies may explain changes in cognition not attributable to GM atrophy.

5.1. Clinical relevance and the road ahead of in vivo synaptic density imaging

Researchers are actively developing synapse-targeted therapies for neurodegenerative disorders (Peng et al., 2022). Preclinical studies suggest potential medications for AD may enhance synaptic density (Kaufman et al., 2015; Smith et al., 2018; Toyonaga et al., 2019). A promising avenue for future exploration is the use of SV2A imaging to monitor therapeutic responses and assess drug efficacy in human clinical trials. Initial progress in this direction has already been made (ID NCT 03493282).

Furthermore, delineating synaptic density pathology onto other imaging markers will provide more profound insights into *how* neurodegenerative diseases progress temporally, as well as elucidate the relative roles and causal relationships of different pathomechanisms (Drzezga et al., 2014). For instance, future research could involve employing structural equation modelling to gain insights into the temporal relationships between Tau, synaptic density, and cognitive impairment. Furthermore, investigating the link between synaptic density decline and Aβ-toxicity could contribute to a more nuanced stratification of patient populations.

Studies with larger patient cohorts, implementing longitudinal approaches starting in preclinical phases, and direct comparisons of clinically resemblant diseases are desired. In pursuit of these objectives, standardising *in vivo* SV2A PET imaging protocols is considered ideal to tackle the ongoing methodological variability in the field and facilitating between-study comparisons. In light of this, it is relevant to further validate newly developed radiotracers, such as the readily available ^{18}F-labeled version of UCB-J, which are more openly available for clinical use. Additionally, validating PVC methods to control for cerebral atrophy is crucial for ensuring accurate and reliable SV2A PET imaging results (Becker et al., 2020; Mercier et al., 2017).

6. Concluding remarks

As a conclusion, SV2A radiotracers have enabled the characterisation of synaptic density loss in the living brain. SV2A PET imaging shows tremendous capability to provide novel insights into the aetiology of neurodegenerative disorders and great promise as a biomarker for synaptic density reduction. Of particular interest herein is its potential contribution to early and differential diagnosis. Furthermore, when combined with other imaging modalities and applied across the spectrum from normal ageing to dementia, SV2A PET imaging may promote efforts to develop disease-modifying therapies that target the preservation and restoration of synapses, making its range of clinical applications immense.

Funding

JOB receives infrastructural support from the Cambridge NIHR BRC. EM is supported by an Alzheimer's Society Junior Research Fellowship (443 AS JF 18017) and Lewy Body Society.

CRediT authorship contribution statement

Malouke Visser conducted the literature searches and wrote the paper. Elijah Mak reviewed the drafts and contributed to the writing of the paper. John O'Brien reviewed the manuscript and provided critical feedback.

Declaration of Generative AI and AI-assisted technologies in the writing process

During the preparation of this work the author(s) used generative AI in order to improve the language and readability of the paper. After using this tool/service, the author(s) reviewed and edited the content as needed and take(s) full responsibility for the content of the publication.

Declaration of Competing Interest

Unrelated to this work, JOB has received honoraria for work as DSMB chair or member for TauRx, Axon, Eisai, has acted as a consultant for Roche, and has received research support from Alliance Medical and Merck.

Data availability

No data was used for the research described in the article.

Appendix A. Supporting information

Supplementary data associated with this article can be found in the online version at doi:10.1016/j.arr.2024.102197.

References

Andersen, K.B., Hansen, A.K., Damholdt, M.F., Horsager, J., Skjaerbaek, C., Gottrup, H., Klit, H., Schacht, A.C., Danielsen, E.H., Brooks, D.J., Borghammer, P., 2021. Reduced synaptic density in patients with lewy body dementia: an [(11) C]UCB-J PET imaging study. Mov. Disord. 36 (9), 2057–2065. https://doi.org/10.1002/mds.28617.

Andersen, K.B., Hansen, A.K., Knudsen, K., Schacht, A.C., Damholdt, M.F., Brooks, D.J., Borghammer, P., 2022. Healthy brain aging assessed with [(18)F]FDG and [(11)C] UCB-J PET. Nucl. Med. Biol. 112-113 (9), 52–58. https://doi.org/10.1016/j.nucmedbio.2022.06.007.

Andersen, K.B., Hansen, A.K., Schacht, A.C., Horsager, J., Gottrup, H., Klit, H., Danielsen, E.H., Poston, K.L., Pavese, N., Brooks, D.J., Borghammer, P., 2023. Synaptic density and glucose consumption in patients with lewy body diseases: an [(11) C]UCB-J and [(18) F]FDG PET study. Mov. Disord. 38 (5), 796–805. https://doi.org/10.1002/mds.29375.

Bastin, C., Bahri, M.A., Meyer, F., Manard, M., Delhaye, E., Plenevaux, A., Becker, G., Seret, A., Mella, C., Giacomelli, F., Degueldre, C., Balteau, E., Luxen, A., Salmon, E., 2020. In vivo imaging of synaptic loss in Alzheimer's disease with [18F]UCB-H positron emission tomography. Eur. J. Nucl. Med. Mol. Imaging 47 (2), 390–402. https://doi.org/10.1007/s00259-019-04461-x.

Becker, G., Dammicco, S., Bahri, M.A., Salmon, E., 2020. The rise of synaptic density PET imaging. Molecules 25 (10). https://doi.org/10.3390/molecules25102303.

Cai, Z., Li, S., Matuskey, D., Nabulsi, N., Huang, Y., 2019. PET imaging of synaptic density: a new tool for investigation of neuropsychiatric diseases. Neurosci. Lett. 691, 44–50. https://doi.org/10.1016/j.neulet.2018.07.038.

Calabresi, P., Ghiglieri, V., Mazzocchetti, P., Corbelli, I., Picconi, B., 2015. Levodopa-induced plasticity: a double-edged sword in Parkinson's disease? Philos. Trans. R. Soc. B 370 (1672). https://doi.org/10.1098/rstb.2014.0184.

Calhoun, M.E., Jucker, M., Martin, L.J., Thinakaran, G., Price, D.L., Mouton, P.R., 1996. Comparative evaluation of synaptophysin-based methods for quantification of synapses. J. Neurocytol. 25 (12), 821–828. https://doi.org/10.1007/BF02284844.

Carapelle, E., Mundi, C., Cassano, T., Avolio, C., 2020. Interaction between cognitive reserve and biomarkers in Alzheimer disease. Int. J. Mol. Sci. 21 (17), 6279. https://doi.org/10.3390/ijms21176279.

Carson, R.E., Naganawa, M., Toyonaga, T., Koohsari, S., Yang, Y., Chen, M.K., Matuskey, D., Finnema, S.J., 2022. Imaging of synaptic density in neurodegenerative disorders. J. Nucl. Med. 63 (Suppl 1), 60S–67S. https://doi.org/10.2967/jnumed.121.263201.

Chen, M.K., Mecca, A.P., Naganawa, M., Finnema, S.J., Toyonaga, T., Lin, S.F., Najafzadeh, S., Ropchan, J., Lu, Y., McDonald, J.W., Michalak, H.R., Nabulsi, N.B., Arnsten, A.F.T., Huang, Y., Carson, R.E., van Dyck, C.H., 2018. Assessing synaptic density in alzheimer disease with synaptic vesicle glycoprotein 2A positron emission tomographic imaging. JAMA Neurol. 75 (10), 1215–1224. https://doi.org/10.1001/jamaneurol.2018.1836.

Chen, M.K., Mecca, A.P., Naganawa, M., Gallezot, J.D., Toyonaga, T., Mondal, J., Finnema, S.J., Lin, S.F., O'Dell, R.S., McDonald, J.W., Michalak, H.R., Vander Wyk, B., Nabulsi, N.B., Huang, Y., Arnsten, A.F., van Dyck, C.H., Carson, R.E., 2021. Comparison of [(11)C]UCB-J and [(18)F]FDG PET in Alzheimer's disease: a tracer kinetic modeling study. J. Cereb. Blood Flow. Metab. 41 (9), 2395–2409. https://doi.org/10.1177/0271678X211004312.

Chen, Z., Liao, G., Wan, N., He, Z., Chen, D., Tang, Z., Long, Z., Zou, G., Peng, L., Wan, L., Wang, C., Peng, H., Shi, Y., Tang, Y., Li, J., Li, Y., Long, T., Hou, X., He, L., Jiang, H., 2023. Synaptic loss in spinocerebellar ataxia type 3 revealed by SV2A positron emission tomography. Mov. Disord. 38 (6), 978–989. https://doi.org/10.1002/mds.29395.

Chetelat, G., Landeau, B., Salmon, E., Yakushev, I., Bahri, M.A., Mezenge, F., Perrotin, A., Bastin, C., Manrique, A., Scheurich, A., Scheckenberger, M., Desgranges, B., Eustache, F., Fellgiebel, A., 2013. Relationships between brain metabolism decrease in normal aging and changes in structural and functional connectivity. NeuroImage 76, 167–177. https://doi.org/10.1016/j.neuroimage.2013.03.009.

Coomans, E.M., Schoonhoven, D.N., Tuncel, H., Verfaillie, S.C.J., Wolters, E.E., Boellaard, R., Ossenkoppele, R., den Braber, A., Scheper, W., Schober, P., Sweeney, S.P., Ryan, J.M., Schuit, R.C., Windhorst, A.D., Barkhof, F., Scheltens, P., Golla, S.S.V., Hillebrand, A., Gouw, A.A., van Berckel, B.N.M., 2021. In vivo tau pathology is associated with synaptic loss and altered synaptic function. Alzheimer'S. Res. Ther. 13 (1), 35 https://doi.org/10.1186/s13195-021-00772-0.

Delva, A., Van Weehaeghe, D., Koole, M., Van Laere, K., Vandenberghe, W., 2020. Loss of Presynaptic Terminal Integrity in the Substantia Nigra in Early Parkinson's Disease. Mov. Disord. 35 (11), 1977–1986. https://doi.org/10.1002/mds.28216.

Delva, A., Van Laere, K., Vandenberghe, W., 2022. Longitudinal positron emission tomography imaging of presynaptic terminals in early Parkinson's disease. Mov. Disord. 37 (9), 1883–1892. https://doi.org/10.1002/mds.29148.

Delva, A., Michiels, L., Koole, M., Van Laere, K., Vandenberghe, W., 2022. Synaptic damage and its clinical correlates in people with early huntington disease: a PET study. Neurology 98 (1), e83–e94. https://doi.org/10.1212/WNL.0000000000012969.

Dierckx, R.A.J.O., Otte, A., de Vries, E.F.J., van Waarde, A., Leenders, K.L., 2021. PET and SPECT in Neurology, 2 ed..,. Springer Nature,, Switzerland.

Drzezga, A., Barthel, H., Minoshima, S., Sabri, O., 2014. Potential clinical applications of PET/MR imaging in neurodegenerative diseases. J. Nucl. Med. 55 (Supplement 2), 47S–55S. https://doi.org/10.2967/jnumed.113.129254.

Dugger, B.N., Dickson, D.W., 2017. Pathology of neurodegenerative diseases. Cold Spring Harb. Perspect. Biol. 9 (7) https://doi.org/10.1101/cshperspect.a028035.

Erlandsson, K., Buvat, I., Pretorius, P.H., Thomas, B.A., Hutton, B.F., 2012. A review of partial volume correction techniques for emission tomography and their applications

in neurology, cardiology and oncology. Phys. Med. Biol. 57 (21), R119–159. https://doi.org/10.1088/0031-9155/57/21/R119.
Fang, X.T., Toyonaga, T., Hillmer, A.T., Matuskey, D., Holmes, S.E., Radhakrishnan, R., Mecca, A.P., van Dyck, C.H., D'Souza, D.C., Esterlis, I., Worhunsky, P.D., Carson, R. E., 2021. Identifying brain networks in synaptic density PET ((11)C-UCB-J) with independent component analysis. NeuroImage 237, 118167. https://doi.org/10.1016/j.neuroimage.2021.118167.
Fang, X.T., Volpi, T., Holmes, S.E., Esterlis, I., Carson, R.E., Worhunsky, P.D., 2023. Linking resting-state network fluctuations with systems of coherent synaptic density: a multimodal fMRI and (11)C-UCB-J PET study. Front. Hum. Neurosci. 17, 1124254 https://doi.org/10.3389/fnhum.2023.1124254.
Feng, G., Xiao, F., Lu, Y., Huang, Z., Yuan, J., Xiao, Z., Xi, Z., Wang, X., 2009. Down-regulation synaptic vesicle protein 2A in the anterior temporal neocortex of patients with intractable epilepsy. J. Mol. Neurosci. 39 (3), 354–359. https://doi.org/10.1007/s12031-009-9288-2.
Finnema, S.J., Nabulsi, N.B., Eid, T., Detyniecki, K., Lin, S.F., Chen, M.K., Dhaher, R., Matuskey, D., Baum, E., Holden, D., Spencer, D.D., Mercier, J., Hannestad, J., Huang, Y., Carson, R.E., 2016. Imaging synaptic density in the living human brain. ra396 Sci. Transl. Med. 8 (348), 348. https://doi.org/10.1126/scitranslmed.aaf6667.
Finnema, S.J., Nabulsi, N.B., Mercier, J., Lin, S.F., Chen, M.K., Matuskey, D., Gallezot, J. D., Henry, S., Hannestad, J., Huang, Y., Carson, R.E., 2018. Kinetic evaluation and test-retest reproducibility of [(11)C]UCB-J, a novel radioligand for positron emission tomography imaging of synaptic vesicle glycoprotein 2A in humans. J. Cereb. Blood Flow. Metab. 38 (11), 2041–2052. https://doi.org/10.1177/0271678X17724947.
Finnema, S.J., Toyonaga, T., Detyniecki, K., Chen, M.K., Dias, M., Wang, Q., Lin, S.F., Naganawa, M., Gallezot, J.D., Lu, Y., Nabulsi, N.B., Huang, Y., Spencer, D.D., Carson, R.E., 2020. Reduced synaptic vesicle protein 2A binding in temporal lobe epilepsy: a [(11) C]UCB-J positron emission tomography study. Epilepsia 61 (10), 2183–2193. https://doi.org/10.1111/epi.16653.
Fujimoto, T., Matsumoto, T., Fujita, S., Takeuchi, K., Nakamura, K., Mitsuyama, Y., Kato, N., 2008. Changes in glucose metabolism due to aging and gender-related differences in the healthy human brain. Psychiatry Res. 164 (1), 58–72. https://doi.org/10.1016/j.pscychresns.2006.12.014.
Gillard, M., Fuks, B., Leclercq, K., Matagne, A., 2011. Binding characteristics of brivaracetam, a selective, high affinity SV2A ligand in rat, mouse and human brain: relationship to anti-convulsant properties. Eur. J. Pharmacol. 664 (1-3), 36–44. https://doi.org/10.1016/j.ejphar.2011.04.064.
Heeman, F., Yaqub, M., Hendriks, J., van Berckel, B.N.M., Collij, L.E., Gray, K.R., Manber, R., Wolz, R., Garibotto, V., Wimberley, C., Ritchie, C., Barkhof, F., Gispert, J.D., Vallez Garcia, D., Lopes Alves, I., Lammertsma, A.A., Consortium, A., 2022. Impact of cerebral blood flow and amyloid load on SUVR bias. EJNMMI Res. 12 (1), 29. https://doi.org/10.1186/s13550-022-00898-8.
Herholz, K., Carter, S.F., Jones, M., 2007. Positron emission tomography imaging in dementia. *Spec No 2*(SPEC. ISS. 2). Br. J. Radiol. 80, S160–167. https://doi.org/10.1259/bjr/97295129.
Holland, N., Jones, P.S., Savulich, G., Wiggins, J.K., Hong, Y.T., Fryer, T.D., Manavaki, R., Sephton, S.M., Boros, I., Malpetti, M., Hezemans, F.H., Aigbirhio, F.I., Coles, J.P., O'Brien, J., Rowe, J.B., 2020. Synaptic loss in primary tauopathies revealed by [(11) C]UCB-J positron emission tomography. Mov. Disord. 35 (10), 1834–1842. https://doi.org/10.1002/mds.28188.
Holland, N., Malpetti, M., Rittman, T., Mak, E.E., Passamonti, L., Kaalund, S.S., Hezemans, F.H., Jones, P.S., Savulich, G., Hong, Y.T., Fryer, T.D., Aigbirhio, F.I., O'Brien, J.T., Rowe, J.B., 2022. Molecular pathology and synaptic loss in primary tauopathies: an 18F-AV-1451 and 11C-UCB-J PET study. Brain: a J. Neurol. 145 (1), 340–348. https://doi.org/10.1093/brain/awab282.
Holland, N., Jones, P.S., Savulich, G., Naessens, M., Malpetti, M., Whiteside, D.J., Street, D., Swann, P., Hong, Y.T., Fryer, T.D., Rittman, T., Mulroy, E., Aigbirhio, F.I., Bhatia, K.P., O'Brien, J.T., Rowe, J.B., 2023. Longitudinal synaptic loss in primary tauopathies: an in vivo [(11) C]UCB-J positron emission tomography study. Mov. Disord. 38 (7), 1316–1326. https://doi.org/10.1002/mds.29421.
Hsieh, T.C., Lin, W.Y., Ding, H.J., Sun, S.S., Wu, Y.C., Yen, K.Y., Kao, C.H., 2012. Sex- and age-related differences in brain FDG metabolism of healthy adults: an SPM analysis. J. Neuroimaging 22 (1), 21–27. https://doi.org/10.1111/j.1552-6569.2010.00543.x.
Hurley, M.J., Jackson, M.J., Smith, L.A., Rose, S., Jenner, P., 2005. Immunoautoradiographic analysis of NMDA receptor subunits and associated postsynaptic density proteins in the brain of dyskinetic MPTP-treated common marmosets. Eur. J. Neurosci. 21 (12), 3240–3250. https://doi.org/10.1111/j.1460-9568.2005.04169.x.
Iaccarino, L., Sala, A., Caminiti, S.P., Perani, D., 2017. The emerging role of PET imaging in dementia. F1000Research 6, 1830. https://doi.org/10.12688/f1000research.11603.1.
Jack, C.R., Jr, Bennett, D.A., Blennow, K., Carrillo, M.C., Dunn, B., Haeberlein, S.B., Holtzman, D.M., Jagust, W., Jessen, F., Karlawish, J., Liu, E., Molinuevo, J.L., Montine, T., Phelps, C., Rankin, K.P., Rowe, C.C., Scheltens, P., Siemers, E., Snyder, H.M., 2018. NIA-AA research framework: toward a biological definition of Alzheimer's disease (Contributors). Alzheimer'S. Dement. 14 (4), 535–562. https://doi.org/10.1016/j.jalz.2018.02.018.
Kaufman, A.C., Salazar, S.V., Haas, L.T., Yang, J., Kostylev, M.A., Jeng, A.T., Robinson, S. A., Gunther, E.C., van Dyck, C.H., Nygaard, H.B., Strittmatter, S.M., 2015. Fyn inhibition rescues established memory and synapse loss in Alzheimer mice. Ann. Neurol. 77 (6), 953–971. https://doi.org/10.1002/ana.24394.
Koole, M., van Aalst, J., Devrome, M., Mertens, N., Serdons, K., Lacroix, B., Mercier, J., Sciberras, D., Maguire, P., Van Laere, K., 2019. Quantifying SV2A density and drug occupancy in the human brain using [(11)C]UCB-J PET imaging and subcortical white matter as reference tissue. Eur. J. Nucl. Med. Mol. Imaging 46 (2), 396–406. https://doi.org/10.1007/s00259-018-4119-8.
Lepeta, K., Lourenco, M.V., Schweitzer, B.C., Martino Adami, P.V., Banerjee, P., Catuara-Solarz, S., de La Fuente Revenga, M., Guillem, A.M., Haidar, M., Ijomone, O.M., Nadorp, B., Qi, L., Perera, N.D., Refsgaard, L.K., Reid, K.M., Sabbar, M., Sahoo, A., Schaefer, N., Sheean, R.K., Seidenbecher, C., 2016. Synaptopathies: synaptic dysfunction in neurological disorders - A review from students to students. J. Neurochem. 138 (6), 785–805. https://doi.org/10.1111/jnc.13713.
Li, S., Naganawa, M., Pracitto, R., Najafzadeh, S., Holden, D., Henry, S., Matuskey, D., Emery, P.R., Cai, Z., Ropchan, J., Nabulsi, N., Carson, R.E., Huang, Y., 2021. Assessment of test-retest reproducibility of [(18)F]SynVesT-1, a novel radiotracer for PET imaging of synaptic vesicle glycoprotein 2A. Eur. J. Nucl. Med. Mol. Imaging 48 (5), 1327–1338. https://doi.org/10.1007/s00259-020-05149-3.
Lu, Y., Toyonaga, T., Naganawa, M., Gallezot, J.D., Chen, M.K., Mecca, A.P., van Dyck, C. H., Carson, R.E., 2021. Partial volume correction analysis for (11)C-UCB-J PET studies of Alzheimer's disease. NeuroImage 238 (April), 118248. https://doi.org/10.1016/j.neuroimage.2021.118248.
Luo, J., Norris, R.H., Gordon, S.L., Nithianantharajah, J., 2018. Neurodevelopmental synaptopathies: Insights from behaviour in rodent models of synapse gene mutations. Prog. Neuro-Psychopharmacol. Biol. Psychiatry 84 (Pt B), 424–439. https://doi.org/10.1016/j.pnpbp.2017.12.001.
Lynch, B.A., Lambeng, N., Nocka, K., Kensel-Hammes, P., Bajjalieh, S.M., Matagne, A., Fuks, B., 2004. The synaptic vesicle protein SV2A is the binding site for the antiepileptic drug levetiracetam [Article]. Proc. Natl. Acad. Sci. 101 (26), 9861–9866. https://doi.org/10.1073/pnas.0308208101.
Mak, E., Holland, N., Jones, P.S., Savulich, G., Low, A., Malpetti, M., Kaalund, S.S., Passamonti, L., Rittman, T., Romero-Garcia, R., Manavaki, R., Williams, G.B., Hong, Y.T., Fryer, T.D., Aigbirhio, F.I., O'Brien, J.T., Rowe, J.B., 2021. In vivo coupling of dendritic complexity with presynaptic density in primary tauopathies. Neurobiol. Aging 101, 187–198. https://doi.org/10.1016/j.neurobiolaging.2021.01.016.
Malpetti, M., Holland, N., Jones, P.S., Ye, R., Cope, T.E., Fryer, T.D., Hong, Y.T., Savulich, G., Rittman, T., Passamonti, L., Mak, E., Aigbirhio, F.I., O'Brien, J.T., Rowe, J.B., 2021. Synaptic density in carriers of C9orf72 mutations: a [(11) C]UCB-J PET study. Ann. Clin. Transl. Neurol. 8 (7), 1515–1523. https://doi.org/10.1002/acn3.51407.
Malpetti, M., Simon Jones, P., Cope, T.E., Holland, N., Naessens, M., Rouse, M.A., Savulich, G., Fryer, T.D., Hong, Y.T., Sephton, S.M., Aigbirhio, F.I., O'Brien, J.T., & Rowe, J.B. (2022). Synaptic loss in behavioural variant frontotemporal dementia revealed by [11C]UCB-J PET. medRxiv. https://doi.org/10.1101/2022.01.30.22270123.
Malpetti, M., Jones, P.S., Cope, T.E., Holland, N., Naessens, M., Rouse, M.A., Rittman, T., Savulich, G., Whiteside, D.J., Street, D., Fryer, T.D., Hong, Y.T., Milicevic Sephton, S., Aigbirhio, F.I., JT, O.B., Rowe, J.B., 2023. Synaptic loss in frontotemporal dementia revealed by [(11) C]UCB-J positron emission tomography. Ann. Neurol. 93 (1), 142–154. https://doi.org/10.1002/ana.26543.
Mansur, A., Rabiner, E.A., Comley, R.A., Lewis, Y., Middleton, L.T., Huiban, M., Passchier, J., Tsukada, H., Gunn, R.N., 2020. Characterization of 3 PET Tracers for Quantification of Mitochondrial and Synaptic Function in Healthy Human Brain: (18)F-BCPP-EF, (11)C-SA-4503, and (11)C-UCB-J. J. Nucl. Med. 61 (1), 96–103. https://doi.org/10.2967/jnumed.119.228080.
Martin, S.L., Uribe, C., & Strafella, A.P. (2023). PET imaging of synaptic density in Parkinsonian disorders. *Journal of Neuroscience Research*. https://doi.org/10.1002/jnr.25253.
Matuskey, D., Tinaz, S., Wilcox, K.C., Naganawa, M., Toyonaga, T., Dias, M., Henry, S., Pittman, B., Ropchan, J., Nabulsi, N., Suridjan, I., Comley, R.A., Huang, Y., Finnema, S.J., Carson, R.E., 2020. Synaptic Changes in Parkinson Disease Assessed with in vivo Imaging. Ann. Neurol. 87 (3), 329–338. https://doi.org/10.1002/ana.25682.
Mecca, A.P., Chen, M.K., O'Dell, R.S., Naganawa, M., Toyonaga, T., Godek, T.A., Harris, J.E., Bartlett, H.H., Zhao, W., Nabulsi, N.B., Wyk, B.C.V., Varma, P., Arnsten, A.F.T., Huang, Y., Carson, R.E., van Dyck, C.H., 2020. In vivo measurement of widespread synaptic loss in Alzheimer's disease with SV2A PET. Alzheimer'S. Dement. 16 (7), 974–982. https://doi.org/10.1002/alz.12097.
Mecca, A.P., O'Dell, R.S., Sharp, E.S., Banks, E.R., Bartlett, H.H., Zhao, W., Lipior, S., Diepenbrock, N.G., Chen, M.K., Naganawa, M., Toyonaga, T., Nabulsi, N.B., Vander Wyk, B.C., Arnsten, A.F.T., Huang, Y., Carson, R.E., van Dyck, C.H., 2022. Synaptic density and cognitive performance in Alzheimer's disease: a PET imaging study with [(11) C]UCB-J. Alzheimer'S. Dement. 18 (12), 2527–2536. https://doi.org/10.1002/alz.12582.
Mecca, A.P., Chen, M.K., O'Dell, R.S., Naganawa, M., Toyonaga, T., Godek, T.A., Harris, J.E., Bartlett, H.H., Zhao, W., Banks, E.R., Ni, G.S., Rogers, K., Gallezot, J.D., Ropchan, J., Emery, P.R., Nabulsi, N.B., Vander Wyk, B.C., Arnsten, A.F.T., Huang, Y., van Dyck, C.H., 2022. Association of entorhinal cortical tau deposition and hippocampal synaptic density in older individuals with normal cognition and early Alzheimer's disease. Neurobiol. Aging 111, 44–53. https://doi.org/10.1016/j.neurobiolaging.2021.11.004.
Mercier, J., Archen, L., Bollu, V., Carre, S., Evrard, Y., Jnoff, E., Kenda, B., Lallemand, B., Michel, P., Montel, F., Moureau, F., Price, N., Quesnel, Y., Sauvage, X., Valade, A., Provins, L., 2014. Discovery of heterocyclic nonacetamide synaptic vesicle protein 2A (SV2A) ligands with single-digit nanomolar potency: opening avenues towards the first SV2A positron emission tomography (PET) ligands. ChemMedChem 9 (4), 693–698. https://doi.org/10.1002/cmdc.201300482.
Mercier, J., Provins, L., Valade, A., 2017. Discovery and development of SV2A PET tracers: potential for imaging synaptic density and clinical applications. Drug Discov. Today.: Technol. 25, 45–52. https://doi.org/10.1016/j.ddtec.2017.11.003.

Mertens, N., Maguire, R.P., Serdons, K., Lacroix, B., Mercier, J., Sciberras, D., Van Laere, K., Koole, M., 2020. Validation of parametric methods for [(11)C]UCB-J pet imaging using subcortical white matter as reference tissue. Mol. Imaging Biol. 22 (2), 444–452. https://doi.org/10.1007/s11307-019-01387-6.

Michiels, L., Delva, A., van Aalst, J., Ceccarini, J., Vandenberghe, W., Vandenbulcke, M., Koole, M., Lemmens, R., Laere, K.V., 2021. Synaptic density in healthy human aging is not influenced by age or sex: a (11)C-UCB-J PET study. NeuroImage 232, 117877. https://doi.org/10.1016/j.neuroimage.2021.117877.

Naganawa, M., Li, S., Nabulsi, N., Henry, S., Zheng, M.Q., Pracitto, R., Cai, Z., Gao, H., Kapinos, M., Labaree, D., Matuskey, D., Huang, Y., Carson, R.E., 2021. First-in-Human Evaluation of (18)F-SynVesT-1, a Radioligand for PET Imaging of Synaptic Vesicle Glycoprotein 2A. J. Nucl. Med 62 (4), 561–567. https://doi.org/10.2967/jnumed.120.249144.

O'Dell, R., Mecca, A., Chen, M.K., Naganawa, M., Toyonaga, T., Lu, Y., Godek, T., Harris, J., Bartlett, H., Banks, E., Kominek, V., Zhao, W., Nabulsi, N., Ropchan, J., Ye, Y., Vander Wyk, B., Huang, Y., Arnsten, A., Carson, R., van Dyck, C., 2021. Association of Aß deposition and regional synaptic density in early Alzheimer's disease: a PET imaging study with [11C]UCB-J. Am. J. Geriatr. Psychiatry 29 (4), S37–S40. https://doi.org/10.1016/j.jagp.2021.01.034.

Page, M.J., Moher, D., Bossuyt, P.M., Boutron, I., Hoffmann, T.C., Mulrow, C.D., Shamseer, L., Tetzlaff, J.M., Akl, E.A., Brennan, S.E., Chou, R., Glanville, J., Grimshaw, J.M., Hrobjartsson, A., Lalu, M.M., Li, T., Loder, E.W., Mayo-Wilson, E., McDonald, S., McKenzie, J.E., 2021. PRISMA 2020 explanation and elaboration: updated guidance and exemplars for reporting systematic reviews. Br. Med. J. 372, n160. https://doi.org/10.1136/bmj.n160.

Peng, L., Bestard-Lorigados, I., Song, W., 2022. The synapse as a treatment avenue for Alzheimer's Disease. Mol. Psychiatry 27 (7), 2940–2949. https://doi.org/10.1038/s41380-022-01565-z.

Rabiner, E.A., 2018. Imaging synaptic density: a different look at neurologic diseases. J. Nucl. Med. 59 (3), 380–381. https://doi.org/10.2967/jnumed.117.198317.

Ritchie, K., Carriere, I., Su, L., O'Brien, J.T., Lovestone, S., Wells, K., Ritchie, C.W., 2017. The midlife cognitive profiles of adults at high risk of late-onset Alzheimer's disease: The PREVENT study. Alzheimer'S. Dement. 13 (10), 1089–1097. https://doi.org/10.1016/j.jalz.2017.02.008.

Rizzoli, S.O., Betz, W.J., 2005. Synaptic vesicle pools. Nat. Rev. Neurosci. 6 (1), 57–69. https://doi.org/10.1038/nrn1583.

Rossano, S., Toyonaga, T., Finnema, S.J., Naganawa, M., Lu, Y., Nabulsi, N., Ropchan, J., De Bruyn, S., Otoul, C., Stockis, A., Nicolas, J.M., Martin, P., Mercier, J., Huang, Y., Maguire, R.P., Carson, R.E., 2020. Assessment of a white matter reference region for (11)C-UCB-J PET quantification. J. Cereb. Blood Flow. Metab. 40 (9), 1890–1901. https://doi.org/10.1177/0271678X19879230.

Rub, U., Seidel, K., Heinsen, H., Vonsattel, J.P., den Dunnen, W.F., Korf, H.W., 2016. Huntington's disease (HD): the neuropathology of a multisystem neurodegenerative disorder of the human brain. Brain Pathol. 26 (6), 726–740. https://doi.org/10.1111/bpa.12426.

Salmon, E., Bahri, M.A., Plenevaux, A., Becker, G., Seret, A., Delhaye, E., Degueldre, C., Balteau, E., Lemaire, C., Luxen, A., Bastin, C., 2021. In vivo exploration of synaptic projections in frontotemporal dementia. Sci. Rep. 11 (1), 16092 https://doi.org/10.1038/s41598-021-95499-1.

Serrano, M.E., Kim, E., Petrinovic, M.M., Turkheimer, F., Cash, D., 2022. Imaging synaptic density: the next holy grail of neuroscience? Front. Neurosci. 16, 796129 https://doi.org/10.3389/fnins.2022.796129.

Smith, L.M., Zhu, R., Strittmatter, S.M., 2018. Disease-modifying benefit of Fyn blockade persists after washout in mouse Alzheimer's model. Neuropharmacology 130, 54–61. https://doi.org/10.1016/j.neuropharm.2017.11.042.

Topcuoglu, E.S., Akdemir, U.O., Atay, L.O., 2022a. What is new in nuclear medicine imaging for dementia. Nöropsikiyatri arşivi 59 (Suppl 1), S17–S23. https://doi.org/10.29399/npa.28155.

Topcuoglu, E.S., Akdemir, U.O., Atay, L.O., 2022b. What is new in nuclear medicine imaging for dementia. Arch. Neuropsychiatry 59 (Suppl 1), S17–S23. https://doi.org/10.29399/npa.28155.

Toyonaga, T., Smith, L.M., Finnema, S.J., Gallezot, J.D., Naganawa, M., Bini, J., Mulnix, T., Cai, Z., Ropchan, J., Huang, Y., Strittmatter, S.M., Carson, R.E., 2019. In vivo synaptic density imaging with (11)C-UCB-J detects treatment effects of saracatinib in a mouse model of Alzheimer disease. J. Nucl. Med 60 (12), 1780–1786. https://doi.org/10.2967/jnumed.118.223867.

Tuncel, H., Boellaard, R., Coomans, E.M., de Vries, E.F., Glaudemans, A.W., Feltes, P.K., Garcia, D.V., Verfaillie, S.C., Wolters, E.E., Sweeney, S.P., Ryan, J.M., Ivarsson, M., Lynch, B.A., Schober, P., Scheltens, P., Schuit, R.C., Windhorst, A.D., De Deyn, P.P., van Berckel, B.N., Golla, S.S., 2021. Kinetics and 28-day test-retest repeatability and reproducibility of [(11)C]UCB-J PET brain imaging. J. Cereb. Blood Flow. Metab. 41 (6), 1338–1350. https://doi.org/10.1177/0271678X20964248.

Tuncel, H., Boellaard, R., Coomans, E.M., Hollander-Meeuwsen, M.D., de Vries, E.F.J., Glaudemans, A., Feltes, P.K., Garcia, D.V., Verfaillie, S.C.J., Wolters, E.E., Sweeney, S.P., Ryan, J.M., Ivarsson, M., Lynch, B.A., Schober, P., Scheltens, P., Schuit, R.C., Windhorst, A.D., De Deyn, P.P., Golla, S.S.V., 2022. Validation and test-retest repeatability performance of parametric methods for [(11)C]UCB-J PET. EJNMMI Res. 12 (1), 3 https://doi.org/10.1186/s13550-021-00874-8.

van Aalst, J., Ceccarini, J., Sunaert, S., Dupont, P., Koole, M., Van Laere, K., 2021. In vivo synaptic density relates to glucose metabolism at rest in healthy subjects, but is strongly modulated by regional differences. J. Cereb. Blood Flow. Metab. 41 (8), 1978–1987. https://doi.org/10.1177/0271678X20981502.

van Waarde, A., Marcolini, S., de Deyn, P.P., Dierckx, R., 2021. PET agents in dementia: an overview. Semin. Nucl. Med. 51 (3), 196–229. https://doi.org/10.1053/j.semnuclmed.2020.12.008.

Vanderlinden, G., Ceccarini, J., Vande Casteele, T., Michiels, L., Lemmens, R., Triau, E., Serdons, K., Tournoy, J., Koole, M., Vandenbulcke, M., Van Laere, K., 2022. Spatial decrease of synaptic density in amnestic mild cognitive impairment follows the tau build-up pattern. Mol. Psychiatry 27 (10), 4244–4251. https://doi.org/10.1038/s41380-022-01672-x.

Vanhaute, H., Ceccarini, J., Michiels, L., Koole, M., Sunaert, S., Lemmens, R., Triau, E., Emsell, L., Vandenbulcke, M., Van Laere, K., 2020. In vivo synaptic density loss is related to tau deposition in amnestic mild cognitive impairment. Neurology 95 (5), e545–e553. https://doi.org/10.1212/WNL.0000000000009818.

Venkataraman, A.V., Mansur, A., Rizzo, G., Bishop, C., Lewis, Y., Kocagoncu, E., Lingford-Hughes, A., Huiban, M., Passchier, J., Rowe, J.B., Tsukada, H., Brooks, D.J., Martarello, L., Comley, R.A., Chen, L., Schwarz, A.J., Hargreaves, R., Gunn, R.N., Rabiner, E.A., & Matthews, P.M. (2022). Widespread cell stress and mitochondrial dysfunction occur in patients with early Alzheimer's disease. Science Translational Medicine, 14(658), eabk1051. https://doi.org/10.1126/scitranslmed.abk1051.

Vonsattel, J.P.G., Keller, C., & Cortes Ramirez, E.P. (2011). Chapter 4 - Huntington's disease – neuropathology. In W. J. Weiner & E. Tolosa (Eds.), Handbook of Clinical Neurology (Vol. 100, pp. 83–100). Elsevier. https://doi.org/https://doi.org/10.1016/B978–0-444–52014-2.00004–5.

Wilson, H., Pagano, G., de Natale, E.R., Mansur, A., Caminiti, S.P., Polychronis, S., Middleton, L.T., Price, G., Schmidt, K.F., Gunn, R.N., Rabiner, E.A., Politis, M., 2020. Mitochondrial Complex 1, Sigma 1, and Synaptic Vesicle 2A in Early Drug-Naive Parkinson's Disease. Mov. Disord. 35 (8), 1416–1427. https://doi.org/10.1002/mds.28064.

Wu, M., Zhang, M., Yin, X., Chen, K., Hu, Z., Zhou, Q., Cao, X., Chen, Z., Liu, D., 2021. The role of pathological tau in synaptic dysfunction in Alzheimer's diseases. Transl. Neurodegener. 10 (1), 45 https://doi.org/10.1186/s40035-021-00270-1.

Yoshizawa, H., Gazes, Y., Stern, Y., Miyata, Y., Uchiyama, S., 2014. Characterizing the normative profile of 18F-FDG PET brain imaging: sex difference, aging effect, and cognitive reserve. Psychiatry Res. 221 (1), 78–85. https://doi.org/10.1016/j.pscychresns.2013.10.009.

Zanderigo, F., Ogden, R.T., Parsey, R.V., 2013. Reference region approaches in PET: a comparative study on multiple radioligands. J. Cereb. Blood Flow. Metab. 33 (6), 888–897. https://doi.org/10.1038/jcbfm.2013.26.

Zhang, H., Schneider, T., Wheeler-Kingshott, C.A., Alexander, D.C., 2012. NODDI: practical in vivo neurite orientation dispersion and density imaging of the human brain. NeuroImage 61 (4), 1000–1016. https://doi.org/10.1016/j.neuroimage.2012.03.072.

Zhang, J., Wang, J., Xu, X., You, Z., Huang, Q., Huang, Y., Guo, Q., Guan, Y., Zhao, J., Liu, J., Xu, W., Deng, Y., Xie, F., Li, B., 2023. In vivo synaptic density loss correlates with impaired functional and related structural connectivity in Alzheimer's disease. J. Cereb. Blood Flow. Metab. 43 (6), 977–988. https://doi.org/10.1177/0271678X231153730.